Pulsed EPR and NMR Spectroscopy of Paramagnetic Iron Porphyrinates and Related Iron Macrocycles: How To Understand Patterns of Spin Delocalization and Recognize Macrocycle Radicals

ARTICLE *in* INORGANIC CHEMISTRY · AUGUST 2003

Impact Factor: 4.76 · DOI: 10.1021/ic026245p · Source: PubMed

1 AUTHOR:

F(rances) Ann Walker
The University of Arizona
240 PUBLICATIONS **8,649** CITATIONS

SEE PROFILE

Inorg. Chem. **2003**, *42*, 4526–4544

Pulsed EPR and NMR Spectroscopy of Paramagnetic Iron Porphyrinates and Related Iron Macrocycles: How To Understand Patterns of Spin Delocalization and Recognize Macrocycle Radicals

F. Ann Walker*

Department of Chemistry, University of Arizona, Tucson, Arizona 85721-0041

Received December 6, 2002

Pulsed EPR spectroscopic techniques, including ESEEM (electron spin echo envelope modulation) and pulsed ENDOR (electron–nuclear double resonance), are extremely useful for determining the magnitudes of the hyperfine couplings of macrocycle and axial ligand nuclei to the unpaired electron(s) on the metal as a function of magnetic field orientation relative to the complex. These data can frequently be used to determine the orientation of the **g**-tensor and the distribution of spin density over the macrocycle, and to determine the metal orbital(s) containing unpaired electrons and the macrocycle orbital(s) involved in spin delocalization. However, these studies cannot be carried out on metal complexes that do not have resolved EPR signals, as in the case of paramagnetic even-electron metal complexes. In addition, the signs of the hyperfine couplings, which are not determined directly in either ESEEM or pulsed ENDOR experiments, are often needed in order to translate hyperfine couplings into spin densities. In these cases, NMR isotropic (hyperfine) shifts are extremely useful in determining the amount and sign of the spin density at each nucleus probed. For metal complexes of aromatic macrocycles such as porphyrins, chlorins, or corroles, simple rules allow prediction of whether spin delocalization occurs through σ or π bonds, and whether spin density on the ligands is of the same or opposite sign as that on the metal. In cases where the amount of spin density on the macrocycle and axial ligands is found to be too large for simple metal–ligand spin delocalization, a macrocycle radical may be suspected. Large spin density on the macrocycle that is of the same sign as that on the metal provides clear evidence of either no coupling or weak ferromagnetic coupling of a macrocycle radical to the unpaired electron(s) on the metal, while large spin density on the macrocycle that is of opposite sign to that on the metal provides clear evidence of antiferromagnetic coupling. The latter is found in a few iron porphyrinates and in most iron corrolates that have been reported thus far. It is now clear that iron corrolates are remarkably noninnocent complexes, with both negative and positive spin density on the macrocycle: for all chloroiron corrolates reported thus far, the balance of positive and negative spin density yields –0.65 to –0.79 spin on the macrocycle. On the other hand, for phenyliron corrolates, the balance of spin density on the macrocycle is zero, to within the accuracy of the calculations (Zakharieva, O.; Schünemann, V.; Gerdan, M.; Licoccia, S.; Cai, S.; Walker, F. A.; Trautwein, A. X. *J. Am. Chem. Soc.* **2002**, *124*, 6636–6648), although both negative and positive spin densities are found on the individual atoms. DFT calculations are invaluable in providing calculated spin densities at positions that can be probed by ^{1}H NMR spectroscopy, and the good agreement between calculated spin densities and measured hyperfine shifts at these positions leads to increased confidence in the calculated spin densities at positions that cannot be directly probed by ^{1}H NMR spectroscopy. ^{13}C NMR spectroscopic investigations of these complexes should be carried out to probe experimentally the nonprotonated carbon spin densities.

NMR and EPR spectroscopic studies of iron porphyrinates and related macrocycles have been of interest to a large number of investigators for many years, in part because of the wide range of interesting magnetic behaviors observed, as well as the importance of understanding the behavior of these metallomacrocycles in biological systems. Except for

* E-mail: awalker@u.arizona.edu.

10.1021/ic026245p CCC: $25.00
Published on Web 07/21/2003

Ann Walker was born and raised in the small town of Adena, Ohio, near Wheeling, West Virginia, in the tristate region of eastern Ohio, the West Virginia panhandle, and western Pennsylvania. In high school, she was very active in music groups, including the marching and concert bands, clarinet quartet, and dance band, at Adena High School. She obtained her B.A. degree in chemistry from The College of Wooster in 1962 and her Ph.D. in physical inorganic chemistry from Brown University in 1966, and she was then an NIH Postdoctoral Fellow with the late Daniel Kivelson at UCLA. Ann began her career as a chemistry professor at Ithaca College in 1967 and moved to San Francisco State University in 1970. She was recipient of an NIH Research Career Development Award for the period 1976−1981. In 1990, she moved to the University of Arizona, where she is currently Regents Professor in the Department of Chemistry, has a joint appointment in the Department of Biochemistry and Molecular Biophysics, and is a member of the Center for Insect Sciences. She teaches undergraduate and graduate courses in inorganic chemistry and magnetic resonance (both NMR and EPR spectroscopy). In 2000, she was recipient of the Garvan−Olin Medal from the American Chemical Society, an award named for Francis P. Garvan and John M. Olin. In 2001, she was recipient of the Luigi Sacconi medal of the Italian Chemical Society, and in late 2002, she received an Alexander von Humboldt Senior Research Fellowship in Science. With this fellowship, she will spend part of her sabbatical year (2003/04) in the Physics Institute at the University of Lübeck, Germany. She will spend another part of her sabbatical year at Stanford University, and the winter in Tucson. Ann is currently an Associate Editor of the *Journal of the American Chemical Society*.

Fe(II) in the presence of strong-field axial ligands, all other oxidation and coordination states of iron macrocycles are paramagnetic, with the number of unpaired electrons ranging from one to six (the presence of six unpaired electrons results in the case of a high-spin Fe(III) center bound to an uncoupled or ferromagnetically coupled macrocycle radical). The unpaired electron(s) on the metal (or also, if present, on the macrocycle) act as "beacon(s)" that "light up" the protons or carbons on the macrocycle and any axial ligands present, by producing hyperfine (or paramagnetic or isotropic) shifts from the expected diamagnetic positions that are proportional to the amount of spin density present at the carbon to which the proton is bound. This property makes it possible, via magnetic resonance investigations, to determine the nature of the orbital(s) involved in spin delocalization, which, in turn, helps to explain the bonding in the complex, since, for the most part, spin delocalization occurs through π symmetry orbitals of the macrocycle and axial ligands.

While most readers of this journal are at least aware that one can observe the proton and carbon resonances of many paramagnetic metal complexes by NMR spectroscopy, many are not aware that pulsed EPR spectroscopy can also be utilized to observe these resonances and thus to learn about the spin density distribution in the macrocycle. In fact, because of the reverse requirements on electron spin relaxation times, pulsed EPR spectroscopy can often be used to observe the nuclei of metal complexes that have electron spin relaxation times that are too long to yield resolved ^{1}H or ^{13}C NMR signals, for example most Cu(II) and all V(IV) complexes.

The purpose of this Viewpoint is to summarize what information can be learned from pulsed EPR and NMR spectroscopy, and how the magnitudes *and signs* of the NMR hyperfine shifts can be utilized to map the pattern of spin density on macrocyclic ligands. The point will be made that the concepts involved are easily comprehended and utilized by researchers at all levels, most importantly by students, who will be the next generation of research scientists. The importance of molecular orbital calculations, even simple orbital symmetry concepts in some cases, in this endeavor will also be emphasized. The concepts developed herein can be generalized to other metals with other d electron configurations, as long as the principles developed herein are followed. Several reviews on NMR spectroscopy of paramagnetic metalloporphyrins have already appeared.[1−5]

For any complex of a transition metal having a partially filled d shell, the electron configuration depends on the crystal field splitting pattern, which is determined by the ligands. Aromatic macrocycles, such as porphyrins, chlorins, isobacteriochlorins, phthalocyanines, corroles, etc., are in general strong-field ligands, but whether their complexes will have the maximum, minimum, or an intermediate number of unpaired electrons depends to a very large degree on the nature and number of axial ligands; many five-coordinate complexes (having only one axial ligand) have the maximum number of unpaired electrons for a given d electron configuration, while many six-coordinate complexes have the minimum number and many four-coordinate complexes have an intermediate number of unpaired electrons. In this Viewpoint, we will concentrate only on iron(III) (d^5) and iron(IV) (d^4), for which the possible spin states are as shown in Figure 1, and on iron(III) macrocycle π cation radicals, which are isoelectronic with Fe(IV) macrocycle complexes but have a different electron configuration. These oxidation and spin states encompass the vast majority of the possible patterns of spin delocalization for all metalloporphyrins. While high-spin d^4 (four unpaired electrons, $S = 2$) is

(1) La Mar, G. N.; Walker, F. A. NMR Studies of Paramagnetic Metalloporphyrins. In *The Porphyrins*; Dolphin, D., Ed.; Academic Press: New York, 1979; Vol. IV, pp 61−157.
(2) Goff, H. M. Nuclear Magnetic Resonance of Iron Porphyrins. In *Iron Porphyrins*; Lever, A. B. P., Gray, H. B., Eds.; Addison-Wesley: Reading, MA, 1983; Part 1, pp 239−281.
(3) Walker, F. A.; Simonis, U. Proton NMR Spectroscopy of Model Hemes. In *Biological Magnetic Resonance, Vol. 12: NMR of Paramagnetic Molecules*; Berliner, L. J., Reuben, J., Eds.; Plenum Press: New York, 1993; pp 133−274.
(4) Walker, F. A. Proton NMR and EPR Spectroscopy of Paramagnetic Metalloporphyrins. In *The Porphyrin Handbook*; Kadish, K. M., Smith, K. M., Guilard, R., Eds.; Academic Press: San Diego, CA; 2000; Vol. 5, Chapter 36, pp 81−183.
(5) Bertini, I.; Luchinat, C.; Parigi, G. *Solution NMR of Paramagnetic Molecules. Applications to Metallobiomolecules and Models*; Elsevier: New York, 2001.

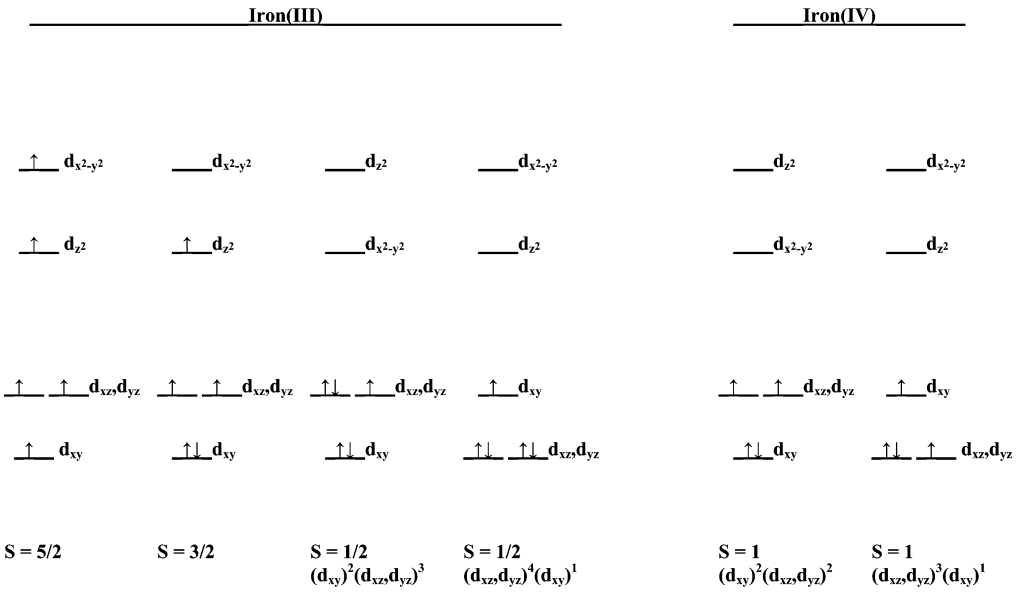

Figure 1. Possible electron configurations for Fe(III) and Fe(IV) porphyrinates.

theoretically possible, to our knowledge there are no examples of iron porphyrinates having this spin state. For both oxidation states, the order of increasing energy of empty orbitals is only hypothetical.

It should be noted that spin *delocalization* indicates the transfer of small fractions of an unpaired electron from the metal to the macrocycle through either L → M or M → L bonding interactions (i.e., covalency of the complex), whereas the existence of a macrocycle radical indicates the *complete removal* of an electron from a π orbital of the macrocycle by one-electron oxidation, or the *complete transfer* of a macrocycle π electron to the metal to yield a complex in which the metal oxidation state is one unit lower and that of the macrocycle is one unit higher than would be the case in the absence of the electron transfer.

Of the five d orbitals whose relative energies are shown schematically in Figure 1, all will be of interest with respect to patterns and magnitudes of spin delocalization to the macrocycle. When the $d_{x^2-y^2}$ orbital is half filled, spin delocalization through σ bonds is observed, which gives rise to large chemical shifts for protons that are only a few chemical bonds from the metal. This applies in particular to high-spin Fe(III) and in principle to high-spin Fe(II) (but see discussion of the pseudocontact shift for HS Fe(II) below), as well as Cu(II) (which is not considered in this Viewpoint, but is discussed in ref 4), the only cases for which the $d_{x^2-y^2}$ orbital is half filled; the β-pyrrole- and *meso*-carbons are each three bonds from the metal, so both can be expected to be affected by σ delocalization of the $d_{x^2-y^2}$ unpaired electron.

In contrast, when the d_{xz} and/or d_{yz} orbitals are half filled, spin delocalization via π orbitals of the macrocycle is observed. This π spin delocalization can occur by means of either ligand-to-metal or metal-to-ligand π donation, depending upon whether the ligand π orbitals are filled or empty, respectively, but in either case, spin is delocalized to the aromatic carbons of the macrocycle. If the macrocycle can distort significantly from planarity, by ruffling, then the d_{xy} orbital may interact with the π system of the macrocycle and thereby cause π spin delocalization to the aromatic carbons of the macrocycle, as well as their attached protons. Finally, for the case of five-coordinate metallo-macrocyclic complexes in which the metal is significantly out of the plane of the four nitrogens, one lobe and the ring of the d_{z^2} orbital of the metal can interact in a symmetry-allowed fashion with the p_π orbitals of all four nitrogens of the macrocycle, as will be described further below.

What orbitals of the macrocycle can be involved in this π spin delocalization? They must be π orbitals that have the proper symmetry and energy to overlap effectively with the d_{xz}, d_{yz}, or, for nonplanar macrocycles, d_{xy} orbitals. For porphyrins, the frontier orbitals are shown in Figure 2,[6,7] where it can be seen that, from orbital symmetry considerations, the 3e(π) filled and 4e(π^*) empty porphyrinate orbitals can interact with the d_{xz} and d_{yz} metal orbitals, while the $3a_{2u}(\pi)$ filled porphyrinate orbital can interact with the metal d_{xy} orbital if the porphyrin ring is ruffled.[8] Viewing the electron density distributions for the 3e(π) filled and 4e(π^*) empty orbitals, we see that there should be significant spin density at the β-pyrrole positions of both sets of orbitals if there are either one or two unpaired electrons in the d_{xz},d_{yz} set, but no spin density at the *meso*-positions if the 3e(π) orbitals are utilized, while there is expected to be some spin density at the *meso*-positions if the 4e(π^*) orbitals are used for spin delocalization. Which set of e-symmetry porphyrin orbitals is utilized by a given metalloporphyrin with unpaired electron(s) in the d_π set will depend on the relative energies of the d_π and two porphyrin frontier e(π) sets. What has been reported in earlier studies is that, for high-spin d^5, the 4e(π^*) set is used[1−4] (although this view is modified by recent DFT calculations that show the symmetry-allowed interaction between the d_{z^2} and $a_{2u}(\pi)$ orbitals when the metal is out of

(6) Based upon the Hückel molecular orbital theory treatment of: Longuet-Higgins, H. C.; Rector, C. W.; Platt, J. R. *J. Chem. Phys.* **1950**, *18*, 1174−1181. The nodal structure (symmetry) of these orbitals is not altered by more recent calculational methods.

(7) *MPORPHW*, an interactive simple Hückel program for Windows, with visualization of the orbitals, their nodal properties, energies, and effect of axial ligand nodal plane is available: http://www.chem.arizona.edu/~shokhirn/nikolai.html.

(8) Safo, M. K.; Walker, F. A.; Raitsimring, A. M.; Walters, W. P.; Dolata, D. P.; Debrunner, P. G.; Scheidt, W. R. *J. Am. Chem. Soc.* **1994**, *116*, 7760−7770. See especially Figure 10.

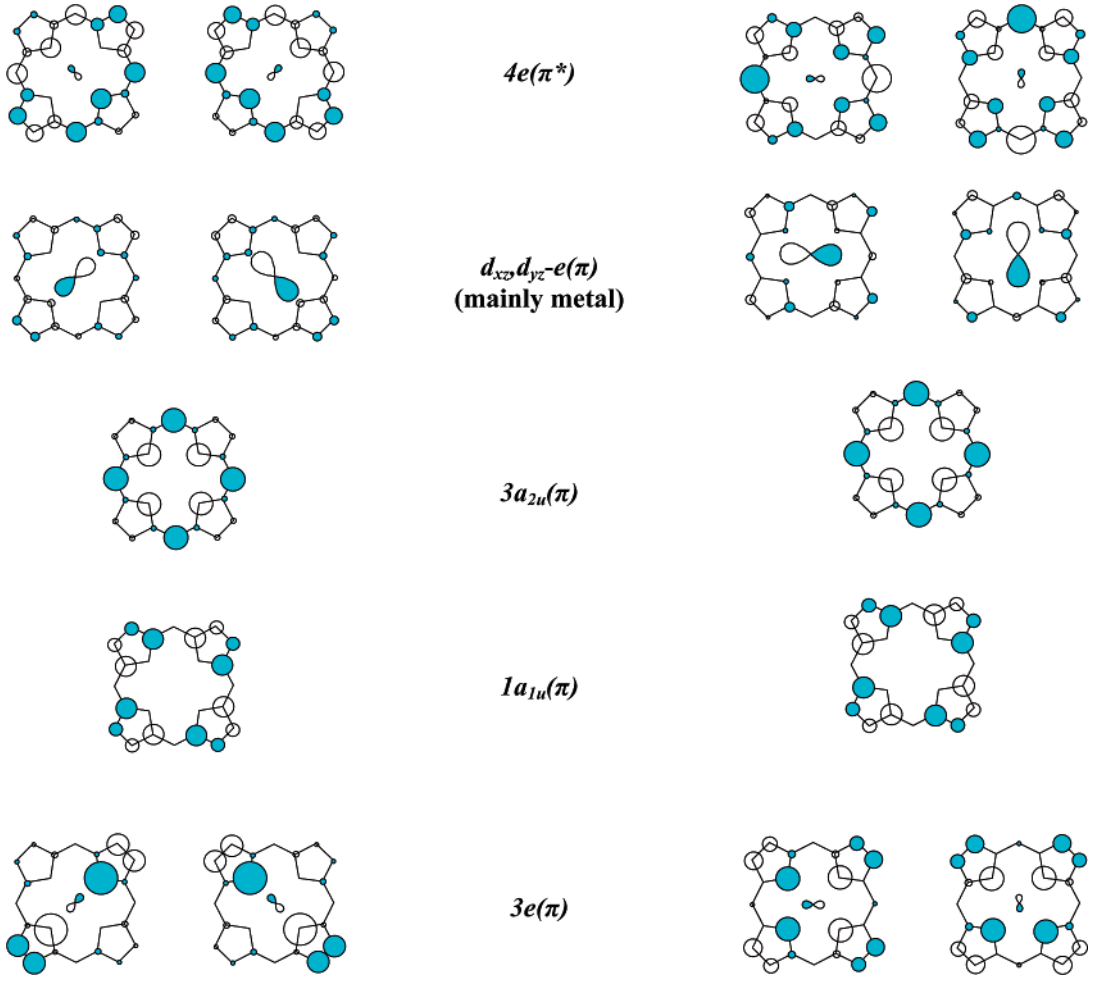

Figure 2. Frontier molecular orbitals of the porphyrin ring, including the mainly metal d_π−e(π) combination orbitals that are usually the HOMOs and/or SOMOs of a metalloporphyrin. Two equivalent representations of the orbitals are shown, with nodes through the nitrogens (left) or the *meso*-positions (right). The relative sizes of the circles at each atom represent the relative orbital electron density coefficients, c_i^2, which should be closely related to spin density coefficients, ρ_C's. Calculated using the program MPORPHW.[7]

the plane; see two paragraphs below), while for low-spin d^5 with a $(d_\pi)^3$ unpaired electron configuration, it is the 3e(π) set.[1−4] (But in fact, there is expected to be a continuum of mixing of varying amounts of each of these sets into the molecular orbitals that contain the unpaired electron(s).) For Fe(IV), on the basis of the lower energies expected for the metal d orbitals for the higher-charged metal, we would expect that the 3e(π) set would be used much more extensively than the 4e(π*) set. Hence, in the extreme cases, for high-spin Fe(III), the mechanism of π spin delocalization is M → Por, with the 4e(π*) set being used, while for low-spin Fe(III) and Fe(IV), the mechanism is Por → M, with the 3e(π) set being used. These cases are totally consistent with the expected energies of the d orbitals with respect to the frontier orbitals of the porphyrinate in each case.

For the case of a single unpaired electron in the d_{xy} orbital of low-spin Fe(III), ruffling of the porphyrinate ring makes possible symmetry-allowed overlap between that orbital and the $3a_{2u}(\pi)$ filled frontier orbital.[8] This orbital has large electron density at both the porphyrinate nitrogens and at the *meso*-carbons, and essentially zero electron density at the β-pyrrole carbons. Hence, delocalization of the unpaired electron from d_{xy} to the $3a_{2u}$ orbital by Por → Fe π donation will lead to large spin density at the *meso*-positions of a ruffled porphyrinate, and practically no spin density at the β-pyrrole positions.

For a five-coordinate metallomacrocyclic complex in which the metal is markedly out of the plane of the four nitrogens of the macrocycle, it has been shown recently that an unpaired electron in the d_{z^2} orbital of the metal can interact with the a_{2u}-type π orbital of the macrocycle. This type of interaction was first shown to lead to antiferromagnetic coupling of the macrocycle radical unpaired electron with the metal d_{z^2} electron in chloroiron corrolates,[9,10] but it has more recently been shown to explain the π spin delocalization from the metal to the *meso*-carbons of (high-spin) chloroiron porphyrinates.[11]

Pulsed EPR Spectroscopy

Although the EPR spectra of paramagnetic iron porphyrinates are too broad to allow direct observation of the hyperfine couplings from the magnetic nuclei near the metal center (^{14}N, ^{1}H, others if labeled), such hyperfine couplings can be observed and investigated via several pulsed EPR techniques, including electron spin echo envelope modulation

(9) Steene, E.; Wondimagegn, T.; Ghosh, A. *J. Phys. Chem. B* **2001**, *105*, 11406−11413; **2002**, *106*, 5312.
(10) Zakharieva, O.; Schünemann, V.; Gerdan, M.; Licoccia, S.; Cai, S.; Walker, F. A.; Trautwein, A. X. *J. Am. Chem. Soc.* **2002**, *124*, 6636−6648.
(11) Cheng, R.-J.; Chen, P.-Y.; Lovell, T.; Liu, T.; Noodleman, L.; Case, D. A. *J. Am. Chem. Soc.* **2003**, *125*, 6774−6783.

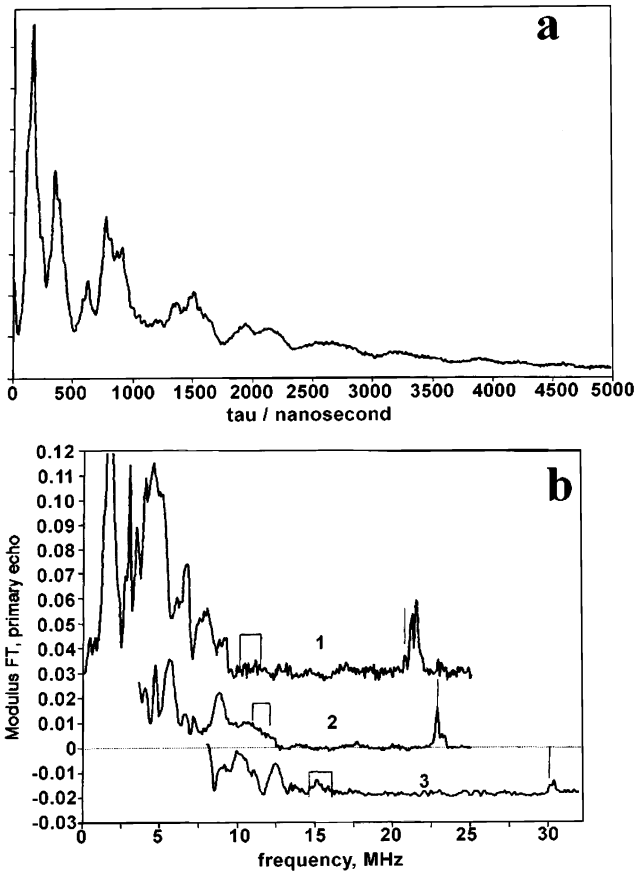

Figure 3. (a) Two-pulse ESEEM time domain data obtained for $[TPPFe(PzH)_2]^+Cl^-$ at a microwave frequency of 8.802 GHz. Other measurement conditions are given in the original publication.[12] (b) FT-ESEEM spectra of the same complex obtained at various magnetic fields: (1) 2440 G; (2) 2680 G; (3) 3550 G. The low-frequency parts of the second and third spectra have been removed in order to avoid overlap with the first. Thin lines show the position of twice the Larmor proton frequency in each case. The peaks at larger frequency than this are shown in this work to be due to the near protons (NPs), the α-H of the axial pyrazole ligands (Figure 4). Open squares mark the expected position of the fundamental frequencies for distant protons (DPs). Reprinted with permission from ref 12. Copyright 1996 American Chemical Society.

(ESEEM) and pulsed electron−nuclear double resonance (ENDOR). These techniques allow one to obtain the spectra due to nuclear transitions that carry the desired information about the hyperfine interactions. In pulsed ENDOR, these spectra are recorded directly as a dependence of the spin−echo signal amplitude on the carrier frequency of the radio frequency pulses irradiating the nuclei. In ESEEM, first, the time domain trace is recorded as a dependence of the spin−echo amplitude on appropriate intervals between the microwave pulses. Then, this time domain trace is Fourier transformed to give the spectrum of nuclear transitions. This spectrum has much in common with the ENDOR spectrum (although, the line shapes are different, and various combination lines may also be present in the ESEEM spectrum). Thus far, our laboratory has concentrated on low-spin Fe(III) macrocycle complexes that give well-resolved EPR signals at 77 K and have long enough electron spin relaxation times at 4.2−10 K to allow ESEEM data to be obtained. An example of the time domain and frequency domain data obtained for the bis(pyrazole) complex of TPPFe(III) in a 1:2 methylene chloride-d_2/toluene-d_8 glass at 4.2 K[12] is shown in Figure 3. The time domain data look somewhat like an

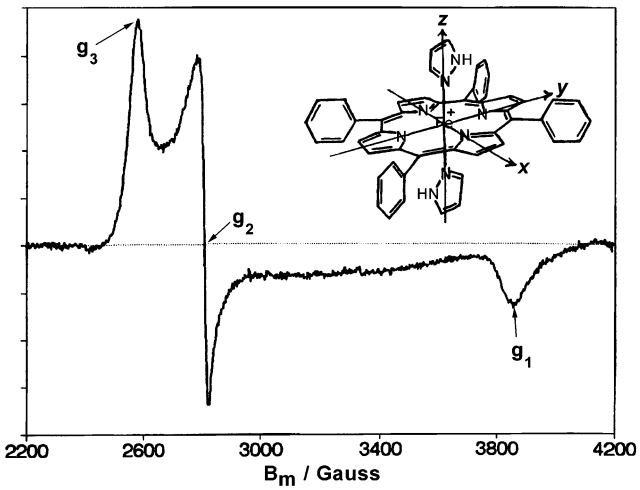

Figure 4. CW EPR spectrum of 10^{-3} M $[TPPFe(PzH)_2]^+Cl^-$ in a 1:2 methylene chloride-d_2/toluene-d_8 glass at 4.2 K: microwave frequency, 9.5529 GHz; power, 0.1 mW. The insert shows the structure of the complex. Observed g-values are $g_3 = 2.60$, $g_2 = 2.38$, and $g_1 = 1.73$. Reprinted with permission from ref 12. Copyright 1996 American Chemical Society.

NMR free-induction decay but contain a nonoscillating background that has to be eliminated numerically before the Fourier transformation. The continuous wave EPR spectrum and structure of the complex are shown in Figure 4.

The frequency domain spectra in Figure 3b were obtained at the turning points of the EPR spectrum located at g_3, g_2, and g_1 (see Figure 4), and thus, they correspond to different orientations of the magnetic field vector with respect to the complex. The spectra include nuclear transitions from different kinds of ^{14}N and ^1H in the complex, and from the ^2H of the solvent (as in ^1H NMR spectroscopy, deuterated solvents are utilized in these studies to avoid interference in observing ^1H signals from the complex). ^{14}N and ^2H give rise to multiple fundamental and combination peaks in the low-frequency region (below 10 MHz in trace 1 and below 14 MHz in trace 3 of Figure 3b). The region around the ^1H Larmor frequency where the protons of the porphyrin and those of the axial ligands contribute is marked in each of the spectra.

As is apparent in traces 1 and 2 of Figure 3b, the peaks in the region of the proton Larmor frequency are practically nonexistent, while in trace 3 a weak broad peak can be seen. The reason for this disappointingly low intensity and low resolution is that the protons in these frozen complexes have different transition frequencies, depending upon the hyperfine interaction parameters, the magnetic field orientation, and the electron spin manifold (α or β). In contrast, at double the Larmor frequency of the proton, $2\nu_I$, two (in traces 2 and 3) or three (in trace 1) resolved and relatively intense signals due to the sum combination frequency, $\nu_+ = \nu_\alpha + \nu_\beta$, can be seen. In the sum combination, the hyperfine interactions contributing to ν_α and ν_β are mostly canceled out, leading to narrow ν_+ lines of considerable intensity located near $2\nu_I$. Importantly, however, the ν_+ frequency is not exactly equal to $2\nu_I$ but is higher than $2\nu_I$ by an amount proportional to the square of the anisotropic hyperfine interaction. Therefore, from the shift of ν_+ lines from $2\nu_I$,

(12) Raitsimring, A. M.; Borbat, P.; Shokhireva, T. Kh.; Walker, F. A. *J. Phys. Chem.* **1996**, *100*, 5235−5244.

one can estimate the anisotropic hyperfine interaction for the protons contributing to these lines.

The exact position of $2\nu_I$ is marked in each trace in Figure 3b, and the peak at this position can be shown to be due to the porphyrin and axial ligand protons that are more than 5 Å from the metal center (referred to as distant protons, DPs). These protons include pyrrole-H at 5.27 Å, phenyl *o*-H at 6.7 Å, and even more distant phenyl protons at *meta*- and *para*-positions, as well as pyrazole β-H at 5.2 Å. The additional ν_+ peaks that occur at higher frequency than $2\nu_I$ can be shown to be due to near protons (referred to as NPs), in this case the N−H and C−H protons α to the bonding nitrogen of the pyrazole ligands, which are approximately 3.1 and 3.3 Å from the metal center, respectively. Hence, of all the protons in the molecule, only the NPs, the axial ligand α-H, exhibit ESEEM signals that are shifted from twice the proton Larmor frequency.

It is found that the intensities of both the NP and DP signals vary as the magnetic field is scanned across the EPR signal (Figure 4). This is because different positions within the *g*-anisotropic EPR spectrum correspond to different orientations of the magnetic field with respect to the complex and, consequently, with respect to the hyperfine interaction tensors of different nuclei. What exactly the magnetic field orientations with respect to the complex will be at each magnetic field (*g*-value) is determined by how the **g**-tensor is oriented relative to the complex. Therefore, the orientation of the **g**-tensor can in principle be established from studying the NP and DP signals (or the nuclear transition spectra in general) as a function of magnetic field. Why may this be important? The measured *g*-values and the equations developed by a number of scientists including Bleaney, Griffith, Taylor, and others,[13−22] that relate the coefficients *a*, *b*, and *c* for the mixing of the three d orbitals, d_{yz}, d_{xz}, and d_{xy}, respectively, under the influence of spin−orbit coupling, allow us to determine in which orbital the unpaired electron of low-spin Fe(III) resides. One of the practical conclusions from those studies is that if the unpaired electron resides mainly in one of the d_π orbitals, d_{xz} or d_{yz}, then the **g**-tensor axis corresponding to the largest principal *g*-value, g_3, should be oriented perpendicular to the plane of the macrocycle. If, on the other hand, the unpaired electron is mostly located in the d_{xy} orbital, then the g_3 axis will be in the macrocycle plane. Thus, if the **g**-tensor orientation with respect to the complex is determined, one can immediately draw conclusions about the d orbital occupied by the unpaired electron, i.e., about the electron configuration of the complex.

For the example shown in Figures 3 and 4, we can calculate theoretically how the NP and DP signal intensities should change for different possible orientations of the **g**-tensor.[12] We take the molecular *z*-axis to be perpendicular to the plane of the porphyrin and the molecular *x*- and *y*-axes to pass through the porphyrin nitrogens, as shown in the picture of the molecule in Figure 4. With such a definition, we seek to determine whether g_1 or g_3 is along the molecular *z*-axis, and then, having accomplished that, how the orientations of the other two *g*-values relate to the *x*- and *y*-axes of the molecule. To learn which *g*-value is aligned along the molecular *z*-axis, we utilize the magnetic field dependence of the DP peak intensity, while to learn about the orientation of the other two axes relative to *x* and *y*, we utilize the magnetic field dependence of the NP peak intensity.

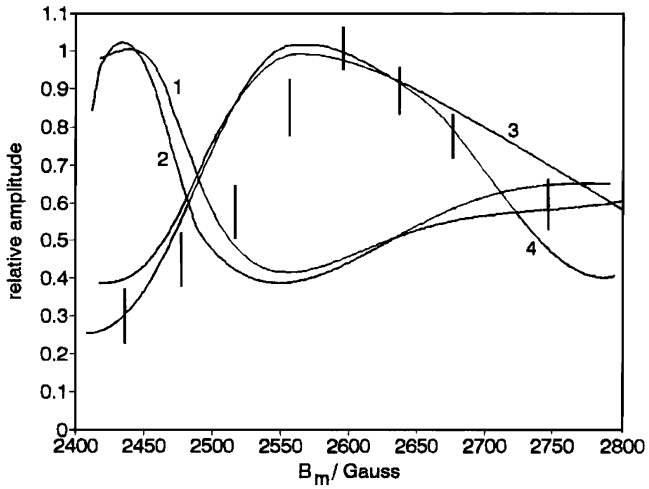

Figure 5. Experimental (bars) and calculated (solid lines) magnetic field strength dependences of the amplitudes of the DP ν_+ peaks. Parameters used for calculations are (curves 1 and 2) $g_{xx} > g_{yy} > g_{zz}$ and (curves 3 and 4) $g_{zz} > g_{yy} > g_{xx}$, and the hyperfine coupling *a* equals 0 MHz for curves 2 and 4 and −1 MHz for curves 1 and 3. Calculations include eight equatorial β-pyrrole protons of the porphyrinate, eight *ortho*-phenyl protons, and four DP protons of the two pyrazole ligands. The planes of both pyrazole rings are aligned along the *x*-axis of the reference coordinate frame. Reprinted with permission from ref 12. Copyright 1996 American Chemical Society.

The magnetic field dependence of the signal intensity of the DP peak (the one at exactly $2\nu_I$) for the case shown in Figure 3 is given by the bars in Figure 5. Two sets each of theoretical fits that are based upon the assignment of the EPR spectrum to the two possible cases, g_1 parallel to *z* (solid lines 1 and 2), and g_3 parallel to *z* (solid lines 3 and 4), are also shown in Figure 5. Comparison of these fits to the experimental data (bars) led to the conclusion that the g_3-axis (corresponding to the largest *g*-value) is along the molecular *z*-axis, and hence, the unpaired electron is mostly localized in one of d_π orbitals.

Obviously, then, the g_2- and g_1-axes lie in the plane of the porphyrin macrocycle.[12] To establish their orientation with respect to the molecular axes *x* and *y*, one can use the so-called counter-rotation property that consists of the following: When the nodal plane of the π system of the axial ligands turns away from the *x*-axis by some angle φ, the g_1-axis turns in the opposite direction from the *x*-axis, also by the angle φ.[23] Thus, if we determine the angle 2φ between the g_1-axis and the plane of the axial ligands, the angle φ will give the orientation of the g_1-axis with respect to *x*. To determine 2φ, we may use the intensities of the NP peaks in the ESEEM spectra in Figure 3b because they belong to the protons of the axial ligands (notably, these protons are in the plane of each ligand). Similar to what was

(13) Bleaney, B.; O'Brien, M. C. M. *Proc. Phys. Soc., London, Sect. B* **1956**, *69*, 1216−1228.
(14) Griffith, J. S. *Nature* **1957**, *180*, 30−31.
(15) Kotani, M. *Suppl. Prog. Theor. Phys.* **1961**, *17*, 4.
(16) Weissbluth, M. *Struct. Bonding* **1967**, *2*, 1−124.
(17) Loew, G. M. H. *Biophys. J.* **1970**, *10*, 196−212.
(18) Griffith, J. S. *Mol. Phys.* **1971**, *21*, 135−139.
(19) Taylor, C. P. S. *Biochim. Biophys. Acta* **1977**, *491*, 137−149.
(20) Bohan, T. L. *J. Magn. Reson.* **1977**, *26*, 109−118.
(21) Rieger, P. H. *Coord. Chem. Rev.* **1994**, *135/136*, 203−286.
(22) McGarvey, B. R. *Coord. Chem. Rev.* **1998**, *170*, 75−92.
(23) Shokhirev, N. V.; Walker, F. A. *J. Am. Chem. Soc.* **1998**, *120*, 981−990.

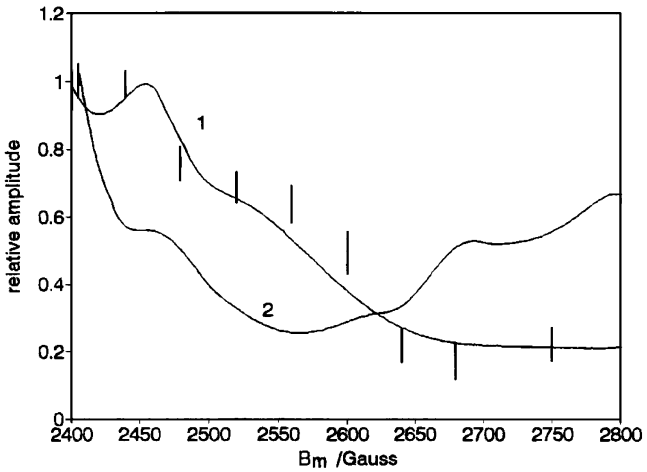

Figure 6. Experimental (bars) and calculated (solid lines) magnetic field strength dependence of the average relative amplitudes of the NP ν_+ peaks. For curve 1, the planes of the pyrazole ligands are parallel, and for curve 2, they are perpendicular to the *x* magnetic axis. Parameters used for calculations are $g_{zz} > g_{yy} > g_{xx}$, Fe−proton distances $r = 3.05$ Å, r−*z*-axis angle of ±43°, and $r = 3.3$ Å, r−*z*-axis angle of ±37°. The isotropic hyperfine coupling constant, *a*, used for the calculated intensity dependence is −0.6 MHz for all NPs. Reprinted with permission from ref 12. Copyright 1996 American Chemical Society.

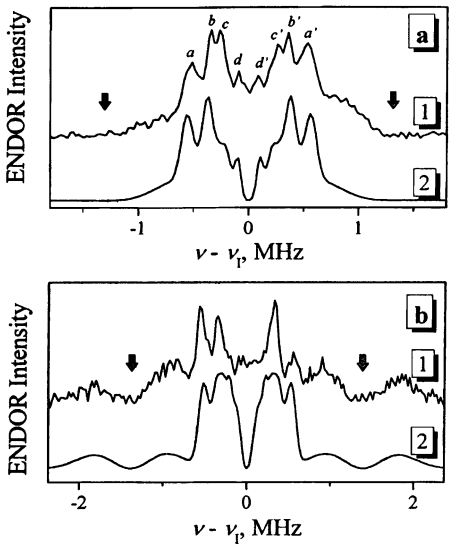

Figure 7. Mims ENDOR spectra (traces 1) of $[TPCFe(Im\text{-}d_4)_2]^+Cl^-$ recorded at (a) g_{LF} ($B_0 = 4320$ G) and (b) g_{HF} ($B_0 = 5960$ G). Measurement conditions are given in the original paper.[27] Arrows indicate blind spots created by the pulse sequence utilized. Trace 2 in each panel is the simulation based upon the hyperfine interaction parameters derived from the spectra. Reprinted with permission from ref 27. Copyright 2001 American Chemical Society.

done for the DP peak (Figure 5), we can calculate the intensities of the NP peaks at various magnetic field positions and compare the calculated dependences with the experimental one shown by bars in Figure 6. Such calculations for various trial values of 2φ show that the experimental and theoretical dependences coincide at $2\varphi \approx 0$ (as an example, see solid lines in Figure 6 showing the calculation results for $2\varphi = 0$ and $2\varphi = 90°$), and thus, both the g_1-axis and the ligand planes are oriented along axis *x* (i.e., along one of the N−Fe−N axes, see Figure 4).

Similar studies of the **g**-tensor and ligand plane orientations have been performed for several low-spin Fe(III) porphyrin complexes,[24−27] including one of a heme protein complex, the histamine complex of nitrophorin 1. In order to obtain useful information about the *g*-frame orientation, and, hence, electron configuration of Fe(III), these studies relied on integral spectroscopic features, like the intensities of DP and NP peaks in the ESEEM spectra. A somewhat different approach to the same problem can be utilized if ENDOR spectroscopy is employed. This approach relies on resolved features in the spectra of nuclear transitions obtained by ENDOR, and on our knowledge of the macrocycle orbitals used for electron spin delocalization in the case of the d_π versus d_{xy} electron configuration of the central ion. We have mentioned above that an unpaired electron in the d_{yz} (and/or d_{xz}) orbital(s) allows spin delocalization to the $3e(\pi)$ orbital(s) while an unpaired electron in the d_{xy} orbital (if the macrocycle is ruffled) allows spin delocalization to the $3a_{2u}(\pi)$ orbital of the porphyrinate ring (Figure 2). Since these two types of π orbitals have opposite patterns of spin delocalization (Figure 2), it should be easy to distinguish between them using the hyperfine interactions of pyrrole protons and protons at *meso*-positions that reflect the spin densities on adjacent carbon atoms. In particular, significant spin density on pyrrole carbons (assessed through the pyrrole-H hyperfine interaction) would indicate the d_{xz}/d_{yz} electron configuration while significant spin density on *meso*-carbons (assessed through a *meso*-H hyperfine interaction) would correspond to the d_{xy} configuration.

To obtain such detailed information about protons, pulsed ENDOR is in general a more suitable technique than ESEEM spectroscopy simply because it tends to accentuate rather than suppress the line shape singularities in the nuclear transition spectra. In addition, it makes possible the direct detection of very broad lines. Applying ENDOR spectroscopy, we observed very broad and featureless signals for the aliphatic protons of the saturated pyrrole ring of $[TPCFe(Im\text{-}d_4)_2]^+$ (see Figure 7) with splittings of up to 4 MHz.[27] The sharper lines with smaller splittings (a−a′, b−b′, c−c′, d−d′) in the ENDOR spectrum of Figure 7a are shown to be due to pyrrole-H (a−a′, b−b′) and phenyl-H (c−c′, d−d′) hyperfine couplings. These assignments and those of the TPP analogue are based on experiments using deuterium labeling of the corresponding TPP complex[28] and on spectral simulations using various spin density distributions obtained by Hückel molecular-orbital calculations.[27] In comparison, the proton ENDOR spectrum of $[TPPFe(Im\text{-}d_4)_2]^+$ exhibits the sharper lines with smaller splittings (a−a′, b−b′, c−c′, d−d′) but does not exhibit the broad lines with large splittings.[27]

The aliphatic β-protons of the pyrroline ring of $[TPCFe(Im\text{-}d_4)_2]^+$ have larger hyperfine couplings than do the protons of the aromatic pyrrole rings of either macrocycle because they report the spin density at the appropriate α-carbon of the pyrroline ring for each β-CH_2 group (rather than the spin density at the β-pyrrole carbon to which the

(24) Raitsimring, A. M.; Walker, F. A. *J. Am. Chem. Soc.* **1998**, *120*, 991−1002.
(25) Astashkin, A. V.; Raitsimring, A. M.; Walker, F. A. *Chem. Phys. Lett.* **1999**, *306*, 9−17.
(26) Schünemann, V.; Raitsimring, A. M.; Benda, R.; Trautwein, A. X.; Shokhireva, T. Kh.; Walker, F. A. *JBIC, J. Biol. Inorg. Chem.* **1999**, *4*, 708−716.
(27) Astashkin, A. V.; Raitsimring, A. M.; Walker, F. A. *J. Am. Chem. Soc.* **2001**, *123*, 1905−1913.
(28) Scholes, C. P.; Falkowski, K. M.; Chen, S.; Bank, J. *J. Am. Chem. Soc.* **1986**, *108*, 1660−1671.

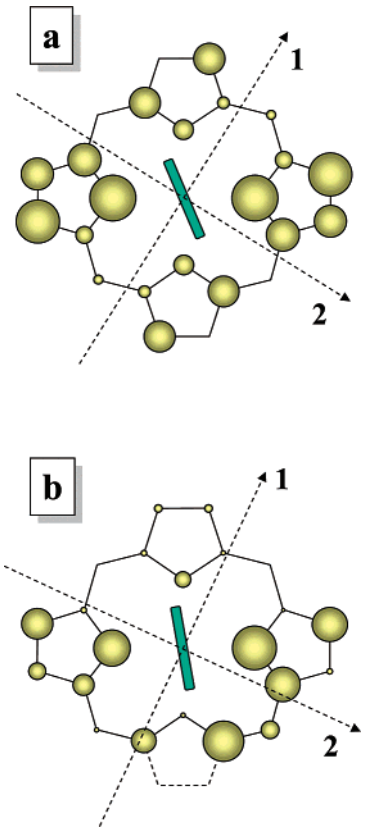

Figure 8. Spin density distributions estimated using Hückel molecular orbital calculations for $[TPPFe(ImH)_2]^+$ (a) and $[TPCFe(ImH)_2]^+$ (b). The rectangle at the center of each tetrapyrrole macrocycle represents the imidazole ligand. The values of φ, the angle from the closest N−Fe−N vector, are 22.5° (a) and 10° (b). The orientations of the **g**-tensor axes 1 and 2 (where 1 = *x*, 2 = *y*) found from analysis of the ENDOR spectra ($\varphi_1 \sim -32°$ in (a) and −25° in (b)) are also shown. Reprinted with permission from ref 27. Copyright 2001 American Chemical Society.

protons are directly attached in the case of the aromatic pyrrole rings of either macrocycle). The spin density in the pyrroline ring is found to be large at the α-carbons, as shown schematically in Figure 8. Appropriate simulations of the expected ENDOR spectra of each complex and comparison to the experimental spectra allow extraction of the hyperfine coupling constants for the β-pyrrole (aromatic) protons of both complexes, which are found to be similar in magnitude, as mentioned above. These calculations yield similar spin density distributions for the low-spin Fe(III) complexes of the porphyrin and the chlorin, leading to the conclusion that each complex utilizes a $3e(\pi)$-type orbital (Figure 2) for delocalization of the unpaired electron from the iron to the macrocycle, i.e., the unpaired electron is mainly in the d_{yz} metal orbital,[27] rather than the iron porphyrin utilizing a $3e(\pi)$ orbital while the iron chlorin utilizes the $3a_{2u}(\pi)$-type orbital, as had been suspected to be the case before this study. ESEEM experiments similar to those discussed above for $[TPPFe(PzH)_2]^+$, for which the intensity data for the NP are plotted in Figure 6, on the complexes in which the imidazole was protonated rather than deuterated allowed determination of the orientation of the *x*- and *y*-axes in these two complexes as well.[27] The results are shown in Figure 8.

More recent investigations of low-spin Fe(III) complexes with isocyanide axial ligands have shown that the *meso*-H hyperfine splitting of $[OEPFe(PhNC)_2]^+$ [29] and the *meso*-^{13}C hyperfine splitting of [*meso*-^{13}C-$TPPFe(t\text{-}BuNC)_2]^+$ [30] are both very large, as expected if the electronic configuration of Fe(III) is d_{xy} and the spin density is delocalized via the $3a_{2u}(\pi)$ orbital of the ruffled macrocycle.

In the above examples, the macrocycle orbitals involved in spin delocalization (and the electronic configuration of the central ion) were identified using the hyperfine couplings obtained by pulsed EPR spectroscopy. The sign of the hyperfine couplings could not be obtained directly in those measurements, but this did not pose any problems because it was possible to discriminate between the candidate orbitals simply based on large or small absolute values of spin densities obtained for β-pyrrole and *meso*-carbons. The signs of these spin densities (and of the related hyperfine couplings) then could be recovered theoretically, from the properties of the particular orbitals (see the next section). However, there are other cases in which it may be extremely important to determine unambiguously the sign of the hyperfine coupling constant, because that sign will tell whether the unpaired electron is delocalized through σ or π bonds, and whether π spin density at the nucleus of interest is positive or negative, and thus whether the spin density on the macrocycle is of the same or opposite sign to that on the metal. To determine the signs of hyperfine coupling constants and spin densities, NMR spectroscopy is the technique of choice, because the *direction* of the paramagnetic shift tells the sign of the hyperfine coupling constant.

^{1}H NMR Spectroscopy of Paramagnetic Iron Macrocycle Complexes

In introducing ^{1}H NMR spectroscopy of paramagnetic complexes, we begin by pointing out that there is no such thing as "paramagnetic NMR" or "diamagnetic NMR" spectroscopy. The spectroscopy is not paramagnetic or diamagnetic: the compounds being studied are! The spectroscopy of diamagnetic and paramagnetic compounds is the same; the compounds being studied differ in that the paramagnetic ones have at least one unpaired electron, and perhaps more than one. This can have consequences in terms of the chemical shifts observed and the relaxation times of the protons of the complex, which means that those who investigate the NMR spectra of paramagnetic complexes must adjust the parameters utilized for obtaining the time domain data and the corresponding frequency domain spectra to values somewhat different than those typically used for diamagnetic compounds, to take account of these differences, but this is not difficult to do: it only requires a little thinking!

In terms of the additional factors that contribute to the chemical shifts of paramagnetic complexes, the observed chemical shifts of the nuclei for such complexes are given by

$$\delta_{obs} = \delta_{dia} + \delta_{para} = \delta_{dia} + \delta_{iso} = \delta_{dia} + \delta_{hf} \qquad (1)$$

where the additional contribution, $\delta_{para} = \delta_{iso} = \delta_{hf}$, and hence the paramagnetic, isotropic, and hyperfine shifts, respectively, represent exactly the same contribution, i.e., that caused by the presence of unpaired electron(s). The

(29) Astashkin, A. V.; Raitsimring, A. M.; Kennedy, A. R.; Shokhireva, T. Kh.; Walker, F. A. *J. Phys. Chem. A* **2002**, *106*, 74−82.
(30) Rivera, M.; Caignan, G. A.; Astashkin, A. V.; Raitsimring, A. M.; Shokhireva, T. Kh.; Walker, F. A. *J. Am. Chem. Soc.* **2002**, *124*, 6077−6089.

paramagnetic, isotropic, or hyperfine contribution to the observed shift is in turn composed of two terms:

$$\delta_{hf} = \delta_{obs} - \delta_{dia} = \delta_{con} + \delta_{pc} \quad (2)$$

where δ_{con} represents the contact (through bond) contribution and δ_{pc} represents the pseudocontact (through space) contribution. Each of these contributions can be estimated with fairly good accuracy.[1−5] For the contact contribution to the hyperfine shift, δ_{con} is expressed in terms of the hyperfine coupling constant, A_h, and the molecular magnetic susceptibilities, χ_{ii}:

$$\delta_{con} = [A_h/3\gamma_N h\beta][\chi_{xx}/g_{xx} + \chi_{yy}/g_{yy} + \chi_{zz}/g_{zz}] \quad (3)$$

where γ_N is the magnetogyric ratio of that nucleus, β is the Bohr magneton, the χ_{ii}-values are the magnetic susceptibilities of the molecule along the three principal magnetic axes, and the g_{ii}-values are the g-values along the same three axes. In the cases where a single spin state with isotropic **g**-tensor is populated (not often the case) and the Curie law is valid, the expression can be simplified to

$$\delta_{con} = A_h <\mathbf{g}> \beta S(S+1)/3\gamma_N hkT \quad (4)$$

where we see clearly the fact that the size of the contact shift varies as a function of inverse temperature. In either case (eq 3 or 4), once A_h has been determined, the McConnell equation is generally used to relate A-values of protons or other nuclei to spin densities:[31]

$$A_H = Q\rho_C/2S \quad (5)$$

where A_H is the hyperfine coupling constant for each individual proton, Q is an empirical constant for a proton or carbon, and ρ_C is the spin density of the electron at the carbon to which the proton is attached. (Similar expressions also exist for A-values of carbons, A_C's, although it is now clear that A_C is very different for the two orbital ground states of low-spin Fe(III) porphyrinates,[30] as can be predicted from the calculations of the contributions to the carbon chemical shifts.[32])

The pseudocontact contribution to the hyperfine or isotropic shift is given by

$$\delta_{pc} = ({}^1/_{12\pi})\{[\chi_{zz} - ({}^1/_2)(\chi_{xx} + \chi_{yy})(3\cos^2\theta - 1)/r^3\} + ({}^3/_2)\{[\chi_{xx} - \chi_{yy}](\sin^2\theta \cos 2\Omega)/r^3\} \quad (6)$$

where χ_{ii}-values are the principal components of the molecular susceptibility tensor in SI units, θ is the angle between the proton−metal vector and the z molecular axis, r is the length of this vector, and Ω is the angle between the projection of this vector on the xy-plane and the x-axis. The terms $(3\cos^2\theta - 1)/r^3$ and $\sin^2\theta \cos 2\Omega)/r^3$ are typically known as the axial and rhombic geometric factors, G_{ax} and G_{rh}, respectively, and can be calculated if the structure of the complex is known. The terms in eq 6 to which they belong are often called the axial and rhombic contributions to the pseudocontact shift, respectively. The pseudocontact shift equation can often be expressed (under the same conditions where the contact shift eq 3 can be simplified to eq 4) as

$$\delta_{pc} = [\mu_0\beta^2 S(S+1)/72\pi kT]\{[2g_{zz}{}^2 - (g_{xx}{}^2 + g_{yy}{}^2)](3\cos^2\theta - 1)r^3 + 3(g_{xx}{}^2 - g_{yy}{}^2)(\sin^2\theta \cos 2\Omega)r^3\} \quad (7)$$

where μ_0 is the permittivity of free space and all other symbols have the same definitions as above.

For nuclei other than protons, there is an additional term that affects the hyperfine shifts of paramagnetic complexes, the ligand-centered pseudocontact shift.[33] This term can be quite large and may scale as the contact shift,[32,33] since it depends on the spin density on the ligand. However, because most of the emphasis in this Viewpoint is on proton hyperfine shifts, the ligand-centered pseudocontact shift will not be discussed further herein.

For all of the spin states of Fe(III), the pseudocontact contribution to the hyperfine shift is much smaller than the contact contribution, and thus for rough estimates of the meaning of the hyperfine shifts, we can consider primarily the contact contribution. (Note: This is not a *necessary* situation that is observed for all paramagnetic complexes;[1−5] in particular, it has been shown not to be the case for high-spin Fe(II) heme centers, where the pseudocontact and contact contributions to the hyperfine shift are comparable in size and of opposite sign, yielding very small observed shifts for ferrocytochrome c'.[34])

There are certain rules as to the relationship between the sign of the contact shift, δ_{con}, and the spin density. These rules have not, to the knowledge of this investigator, ever been violated. They are described in the following paragraph.

For spin density delocalized from the metal d_π orbitals to the ligand protons via ligand π orbitals, A_H is negative ($Q \sim -63$ MHz), and so is the hyperfine shift (see eq 4). This is because of favorable exchange interaction between the π unpaired electron and the σ electron of the C−H bond that has the same spin, leaving the opposite-spin electron on average nearer the nucleus of the hydrogen atom,[31] as shown in Figure 9a. According to the McConnell relation (eq 5), this represents the delocalization of *positive* spin density from the metal d orbitals to the ligand carbons. Hence, protons attached to carbons that are part of aromatic rings that are involved in direct π spin delocalization from the metal to the macrocycle will have *negative* hyperfine shifts,[31] and likely also *negative* chemical shifts, assuming that the diamagnetic shifts are smaller than the hyperfine shifts (eq 1). This applies to protons bound directly to either the β-pyrrole or *meso*-carbons of porphyrinate ligands and related macrocycles, whether the metal orbitals utilized are d_π (d_{xz} and d_{yz}) (for a planar macrocycle) or d_{xy} (for a ruffled or in some cases saddled macrocycle). Examples of this behavior include the pyrrole protons of $[TPPFe(ImH)_2]^+$, as shown in Figure 10A, and the *meso*-protons of $[OEPFe(t\text{-}BuNC)_2]^+$, as shown in Figure 10B. If an aliphatic carbon is inserted

(31) Carrington, A.; McLachlan, A. D. *Introduction to Magnetic Resonance*; Harper & Row: New York, 1967; pp 80−83.
(32) Goff, H. M. *J. Am. Chem. Soc.* **1981**, *103*, 3714−3722.
(33) Mispelter, J.; Momenteau, M.; Lhoste, J.-M. Heteronuclear Magnetic Resonance Applications to Biological and Related Paramagnetic Molecules. In *Biological Magnetic Resonance, Vol. 12: NMR of Paramagnetic Molecules*; Berliner, L. J., Reuben, J., Eds.; Plenum Press: New York, 1993; pp 299−355.
(34) Bertini, I.; Dikiy, A.; Luchinat, C.; Macinai, R.; Viezzoli, M. S. *Inorg. Chem.* **1998**, *37*, 4814−4821.

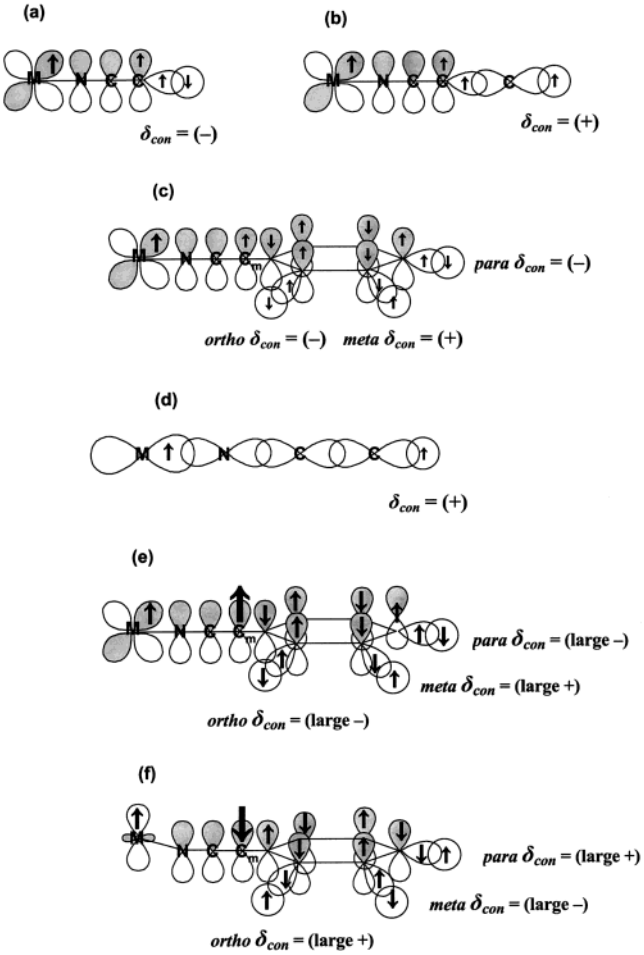

Figure 9. Signs of the spin density present at a proton of interest[31] for several cases of interest: (a) π spin delocalization to the carbon to which the proton is attached (either β-pyrrole or *meso*); (b) the effect of insertion of an aliphatic carbon into the C−H bond of (a) (either β-pyrrole or *meso*); (c) the effect of insertion of a phenyl ring into the *meso*-C−H bond;[39,40] (d) σ spin delocalization to the carbon to which the proton is attached (either β-pyrrole or *meso*); (e) a macrocycle radical in which the macrocycle unpaired electron (large arrow) is uncoupled or weakly feromagnetically coupled to the metal unpaired electron; and (f) a macrocycle radical in which the macrocycle unpaired electron (large arrow) is antiferromagnetically coupled to the metal unpaired electron. Nodal properties of the individual π orbitals are not included in these drawings.

between the aromatic ring and the proton of interest, then the direction of the shift is found to be reversed; i.e., the hyperfine shift is *positive* (Figure 9b), as shown by the pyrrole-CH_2 protons of $[OEPFe(ImH)_2]^+$, as shown in Figure 10C. Whether or not the *magnitude* of the hyperfine shift of the pyrrole-CH_n is reduced over that of the pyrrole-H depends on whether the aliphatic carbon is a methyl group (which spins freely) or a larger alkyl group, as in the case of an ethyl group, where preferred orientations of the methylene protons may lead to larger or smaller isotropic shifts of protons than might have been expected. In fact, while the McConnell *Q*-value for methyl protons is taken as +70 to +75 MHz,[35,36] the *Q*-value for methylene protons can vary from nearly 0 to +100 MHz[37] and can be temperature dependent if rotation of the alkyl group becomes more free at higher temperatures. In any case, a clear sign of π spin delocalization to a particular carbon atom is that a proton

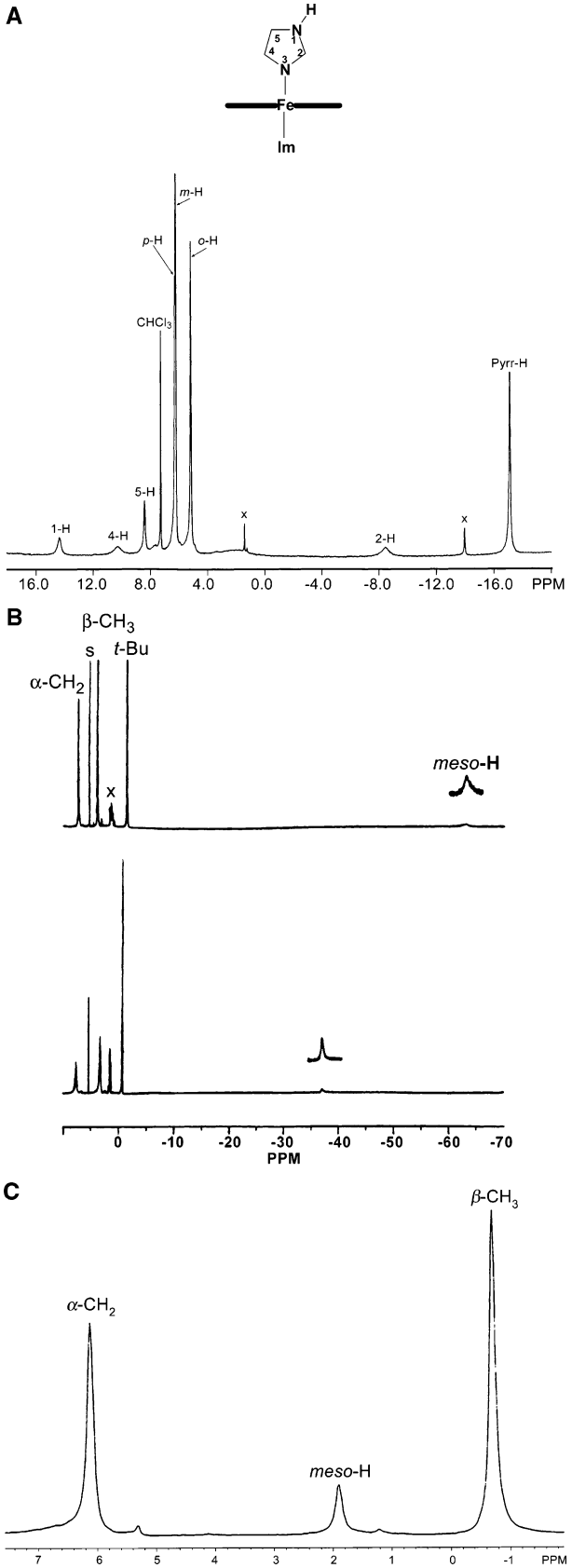

Figure 10. (A) 1D ^{1}H NMR spectrum of $[TPPFe(ImH)_2]^+$ in CD_2Cl_2, recorded at −20 °C. (B) 1D ^{1}H NMR spectrum of $[OEPFe(t\text{-}BuNC)_2]^+$ in CD_2Cl_2, recorded at 30 (bottom) and −78 (top) °C. (C) 1D ^{1}H NMR spectrum of $[OEPFe(Im\text{-}d_4)_2]^+$ in CD_2Cl_2, recorded at 0 °C. (A) Taken from L. Yatsunyk, unpublished work. (B) Reprinted with permission from ref 46. Copyright 1996 American Chemical Society. (C) Taken from S. Cai, unpublished work.

(35) McLachlan, A. D. *Mol. Phys.* **1958**, *1*, 233−240.
(36) Chestnut, D. B. *J. Chem. Phys.* **1958**, *29*, 43−47.

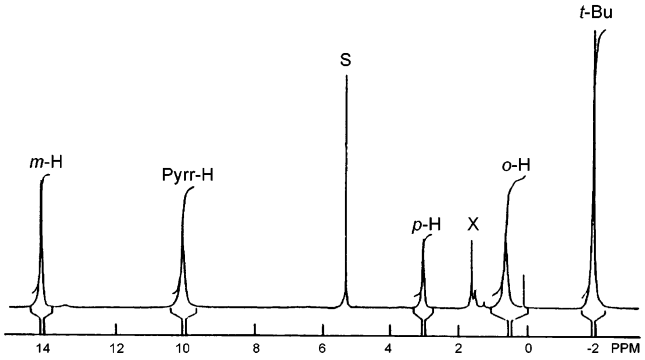

Figure 11. 1D ^{1}H NMR spectrum of $[TPPFe(t\text{-}BuNC)_2]^+ClO_4^-$ in CD_2Cl_2 at 298 K.[38] The peak assignments are marked. Reprinted with permission from ref 38. Copyright 1989 American Chemical Society.

directly attached to this carbon will have a negative hyperfine shift,[31] but if an aliphatic carbon is inserted between this carbon and the proton, then the sign of the hyperfine shift of the proton will reverse and the proton resonance will appear at a positive chemical shift. This is shown schematically in Figure 9a,b, and experimentally in Figure 10A,C.

meso-Phenyl-H shifts of metal complexes of tetraphenylporphyrin (TPP), tetraphenylchlorin (TPC), and triphenylcorrole (TPCorr) are particularly interesting and extremely informative in cases where there is significant spin density at the *meso*-carbons of a macrocycle having phenyl groups at those positions, especially as in the cases of the $(d_{xy})^1$ ground state complexes of low-spin Fe(III), and the iron corrolates. These phenyl-H shifts have not been utilized to their fullest potential in the past, and thus, they are emphasized in this Viewpoint. In cases where there is significant spin density at the *meso*-carbons of a macrocycle, it is found that the sign of the hyperfine or isotropic shift of phenyl protons alternates, with *o*-H and *p*-H shifts being negative and *m*-H shifts positive, as shown in Figure 11 for $[TPPFe(t\text{-}BuNC)_2]^+$,[38] and schematically in Figure 9c. An explanation for this behavior is found in the EPR literature of the 1950s and 1960s, where studies of aromatic radicals such as the benzyl radical showed alternating signs for their hyperfine couplings. These radicals are called "odd-alternant hydrocarbon fragments" because they have odd numbers of carbons involved in π spin delocalization, and because they were shown many years ago to exhibit alternating-sign spin densities, with positive spin densities on the methylene and *ortho*- and *para*-carbons, and negative spin density on the quaternary and *meta*-carbons.[39,40] Somewhat more recently, it was found that, in the NMR spectra of metallotetraphenylporphyrins, the *meso*-carbon appears to play the role of the methylene carbon of the benzyl radical, and the carbons of the phenyl ring similarly behave as those in the benzyl radical, as odd-alternant hydrocarbon fragments.[41] Hence, the positive shift of the *meta*-H and negative shifts of the *ortho*-H and *para*-H of $[TPPFe(t\text{-}BuNC)_2]^+$, shown in Figure 11, are in complete accord with expectations on the basis of treating them as odd-alternant hydrocarbon fragments, and these shifts indicate negative spin density at the *meta*-carbons and positive spin density at the *ortho*- and *para*-carbons of the phenyl ring (Figure 9c). Thus, the observation of alternating signs for the shifts of the phenyl protons indicates large spin density at the *meso*-carbons, as recognized by Simonneaux and co-workers in the first report of the NMR spectrum of this complex[38] (Figure 11).

Thus, for *meso*-phenyl-substituted macrocycles such as tetraphenylporphyrins or tetraphenylchlorins that have metal d electron configurations that produce large amounts of *positive* spin density at the *meso*-carbons (i.e., the same sign as the spin on the metal), the difference in the chemical shifts of the phenyl protons (protons attached directly to a phenyl ring), $\delta_m - \delta_p$, and $\delta_m - \delta_o$, are both *large and positive*, as clearly predicted by Figure 9c. In contrast, for the same *meso*-phenyl-substituted macrocycles that have metal d electron configurations that produce little or no spin density at the *meso*-carbons, the difference in the chemical shifts of the phenyl protons, $\delta_m - \delta_p$, and $\delta_m - \delta_o$, are *small*, with $\delta_m - \delta_p$ positive and $\delta_m - \delta_o$ usually negative because there is no contact shift and thus the chemical shifts follow the expectations of the pseudocontact contribution to the hyperfine shift, plus the ring-current shift difference for *ortho*- and *meta*-H (metal-free macrocycle $\delta_m - \delta_o \sim -0.5$ to -0.7 ppm); the pseudocontact shift of the *ortho*-H is always larger in magnitude than that of the *meta*- and *para*-H.

For spin density delocalized from the metal d_σ orbital appropriate for interaction with the macrocycle ($d_{x^2-y^2}$ in the case of the porphyrin ring, or d_{xy} in the case of the chlorin or corrole rings), to the macrocycle protons via σ orbitals, A_H is *positive*,[31] and so is the hyperfine shift. There is no corresponding McConnell *Q*-value (eq 5) that is widely accepted in the case of σ spin delocalization, because there have not been enough examples studied where there is σ spin delocalization in the absence of π spin delocalization, but nevertheless, the hyperfine shifts of such protons are large and positive. This represents the delocalization of *positive* spin density from the metal d_σ orbital to the macrocycle carbons and their attached protons, and it attenuates rapidly as the number of bonds between the metal and the protons of interest increases. Hence, protons attached to carbons that are involved in σ spin delocalization from the metal to the macrocycle will have *positive* hyperfine shifts, and *positive* chemical shifts. This is shown schematically in Figure 9d. Insertion of an aliphatic carbon reduces the size of the positive shift.

In the case of either σ or π spin delocalization, the observed shifts are very dependent upon temperature, because the hyperfine or isotropic shifts of resonances in homogeneous solution result from the fact that electron spin relaxation is fast enough to average the chemical shifts of the $-^1/_2$ and $+^1/_2$ electron spin components of the hyperfine-split proton resonances[42,43] that would be seen in the ENDOR

(37) There is a modified McConnell equation that covers these situations: $A_H = Q_{CH_2R}\rho_C/2S = (B_0 + B_2\cos^2\varphi)\rho_C/2S$ where B_0 and B_2 are positive parameters and φ is the angle between the C−C−H plane and the p_z orbital axis on the aromatic carbon. B_2 is usually small, and since $\cos^2\varphi$ is positive for all angles φ, Q_{CH_2R} is always positive.[31]

(38) Simonneaux, G.; Hindre, F.; Le Plouzennec, M. *Inorg. Chem.* **1989**, *28*, 823−825.
(39) McLachlan, A. D. *Mol. Phys.* **1960**, *3*, 233−252.
(40) Carrington, A.; McLachlan, A. D. *Introduction to Magnetic Resonance*; Harper & Row: New York, 1967; pp 91−93.
(41) La Mar, G. N.; Del Gaudio, J.; Frye, J. S. *Biochim. Biophys. Acta* **1977**, *498*, 422−435.
(42) Bertini, I.; Luchinat, C. Nuclear Magnetic Resonance of Paramagnetic Substances in Solution. In *Physical Methods for Chemists*, 2nd ed.; Drago, R. S., Ed.; Saunders College Publishing, Harcourt Brace Jovanovich College Publishers: San Diego, CA; 1977; Chapter 12.
(43) Banci, L. Nuclear Relaxation in Paramagnetic Metalloproteins. In *Biological Magnetic Resonance, Vol. 12, NMR of Paramagnetic Molecules*; Berliner, L. J., Reuben, J., Eds.; Plenum: New York, 1993; Chapter 2.

spectra of frozen samples at low temperatures, an average which depends on the Boltzmann populations of the two electron spin components (and rapid interchange between them).[1−5,42,43] Thus, the hyperfine shifts of the averaged resonances depend on temperature according to the Curie law

$$\delta_{hf} \propto (A_h + C_{pc})/T \quad (8)$$

as shown by eqs 4 and 7 above.[44] If there is a thermally accessible excited state that has a different spin density distribution and/or a different orientation of the magnetic axes that give rise to the pseudocontact shift, then there may be some curvature to the plot of δ_{hf} versus $1/T$.[45] In any case, it is extremely important that the *temperature of the measurement of NMR spectra* of paramagnetic complexes be reported, since resonances can move dramatically as a function of temperature,[46] as is evident in Figure 10B and the chemical shift data from many other of the publications quoted herein.

Beyond the differences in chemical shifts, and their temperature dependence, it should also be mentioned that the unpaired electron(s) on the metal cause shortened relaxation times, T_1 and T_2, of the macrocycle protons, which cause the resonances to be broader than typically observed for diamagnetic compounds. T_1 and T_2 values are extremely valuable in determining how far a given proton is from a paramagnetic center, and each can be utilized within the proper theoretical framework. Although detailed discussion of the use of T_1 and T_2 values in structure determination is beyond the scope of this paper, we have applied it to the assignment of the pyrrole protons in a Mo(V)-appended derivative of $[TPPFe(NMeIm)_2]^+$.[47] More detailed discussion of the measurement and analysis of T_1 and T_2 relaxation times, and their use in the study of paramagnetic complexes, is found in refs 42 and 43.

The above principles are well illustrated by (and were originally developed from) the example data provided in Table 1. Specifically, beginning with high-spin Fe(III), with an unpaired electron in each of the five d orbitals, the pyrrole-H shift of the TPPFeCl complex is large and positive because of the d_σ ($d_{x^2-y^2}$ in this case) unpaired electron.[1−4] It should be noted that this large positive chemical shift (+81 ppm at 25 °C[48]) must be the balance of the contributions of the d_σ and d_π unpaired electrons, and so, on the basis of the negative shift observed for the "pure" $S = {}^3/_2$ complexes discussed at the end of the next paragraph, we might expect that the positive shift is reduced by about 50 ppm at ambient temperatures due to the negative shift contribution of the two d_π unpaired electrons also present in this high-spin Fe(III) complex. In other words, although we cannot measure it directly, the chemical shift of the pyrrole-H due to the d_σ unpaired electron alone may be around +130 ppm at 25 °C. (However, this is a much larger value than that measured for CuTPP (+41 ppm at 25 °C),[49] probably because of less favorable interaction between the $d_{x^2-y^2}$ unpaired electron of the +2 metal with the porphyrin nitrogen σ orbitals.) The *meso*-phenyl-H shift differences for this complex, $\delta_m - \delta_p$ and $\delta_m - \delta_o$, are small but both positive, suggesting some π spin density at the *meso*-carbons, as expected for d_π spin delocalization to the 4e(π*) orbitals (Figure 2). A very similar pattern is found for the chlorin complex, TPCFeCl[50] (Table 1). This positive spin density at the *meso*-carbons has recently been explained by spin delocalization from the d_{z^2} orbital of the out-of-plane metal to the $a_{2u}(\pi)$-type orbital of the macrocycle by macrocycle → Fe π donation,[11] rather than delocalization to the *meso*-carbons via π donation of the d_{xz} and d_{yz} unpaired electrons to the 4e(π*)-type empty orbitals of the macrocycle (Figure 2), as suggested previously.[1−4]

For six-coordinate high-spin Fe(III) complexes such as $[TPPFe(DMSO)_2]^+ClO_4^-$, the pattern is somewhat different. The pyrrole-H chemical shift is slightly smaller (+73 ppm at 295 K[51] instead of +81 ppm[48]), and the *meso*-phenyl-H shift differences $\delta_m - \delta_p$ and $\delta_m - \delta_o$ are both small and negative[51] (Table 1), possibly indicative of small negative spin density at the *meso*-positions. This has not yet been investigated in detail, but it is clear that the same $d_{z^2}-a_{2u}(\pi)$-type pathway[11] is not available in this case, because the iron is in the plane of the macrocycle. Therefore, another explanation of the negative *meso*-phenyl-H shift differences will have to be found.

For the spin-admixed $S = {}^5/_2,{}^3/_2$ OETPPFeCl[52] and $TPPFeClO_4$[53−55] complexes, both the pyrrole-H shift and $\delta_m - \delta_p$, and $\delta_m - \delta_o$, decrease as the amount of $S = {}^3/_2$ contribution increases, with both positive and negative pyrrole-H shifts having been reported, depending on whether the $S = {}^5/_2$ or $S = {}^3/_2$ contribution dominates. Furthermore, the temperature dependence of the pyrrole-H resonances of spin-admixed iron porphyrinates can vary wildly.[55]

In contrast, for "pure" $S = {}^3/_2$ complexes, such as $[(2,4,6\text{-}(OCH_3)_3)_4TPPFe(THF)_2]^+ClO_4^-$ or the five-coordinate perchlorate complex of the same porphyrinate,[56] the pyrrole-H shift is negative, as expected when there is not an unpaired electron in the $d_{x^2-y^2}$ orbital, yet the two d_π orbitals, d_{xz} and d_{yz}, each contain an unpaired electron. The larger negative pyrrole-H shifts for these complexes (∼ −30 ppm at 25 °C,[55,56] Table 1), as compared to those for the low-spin Fe(III) complexes having the $(d_{xy})^2(d_{xz},d_{yz})^3$ electronic ground state (∼ −16 ppm), discussed in the next paragraph, are totally in line with expectations, on the basis of the dominance of the contact shift and the presence of two d_π unpaired

(44) This is not strictly true for HS Fe(III), where the pseudocontact shift is proportional to the zero-field splitting constant D, and inversely proportional to the square of the temperature, $\delta \propto D/T^2$.[1−4]

(45) Shokhirev, N. V.; Walker, F. A. *J. Phys. Chem.* **1995**, *99*, 17795−17804.
(46) Walker, F. A.; Nasri, H.; Turowska-Tyrk, I.; Mohanrao, K.; Watson, C. T.; Shokhirev, N. V.; Debrunner, P. G.; Scheidt, W. R. *J. Am. Chem. Soc.* **1996**, *118*, 12109−12118.
(47) Basu, P.; Shokhirev, N. V.; Enemark, J. H.; Walker, F. A. *J. Am. Chem. Soc.* **1995**, *117*, 9042−9055.
(48) Cheng, R.-J.; Latos-Grazynski, L.; Balch, A. L. *Inorg. Chem.* **1982**, *21*, 2412−2418.
(49) Godziela, G. M.; Goff, H. M. *J. Am. Chem. Soc.* **1986**, *108*, 2237−2243.
(50) Pawlik, M. J.; Miller, P. K.; Sullivan, E. P., Jr.; Levstik, M. A.; Almond, D. A.; Strauss, S. H. *J. Am. Chem. Soc.* **1988**, *110*, 3007−3012.
(51) Yatsunyk, L. Unpublished work.
(52) Ogura, H.; Yatsunyk, L.; Medforth, C. J.; Smith, K. M.; Barkigia, K. M.; Renner, M. W.; Melamed, D.; Walker, F. A. *J. Am. Chem. Soc.* **2001**, *123*, 6564−6578.
(53) Boersma, A. D.; Goff, H. M. *Inorg. Chem.* **1982**, *21*, 581−586.
(54) Goff, H. M.; Shimomura, E. *J. Am. Chem. Soc.* **1980**, *102*, 31−37.
(55) Nesset, M. J. M.; Cai, S.; Shokhireva, T. Kh.; Shokhirev, N. V.; Jacobson, S. E.; Jayaraj, K.; Gold, A.; Walker, F. A. *Inorg. Chem.* **2000**, *39*, 532−540.
(56) Toney, G. E.; terHaar, L. W.; Savrin, J. E.; Gold, A.; Hatfield, W. E.; Sangaiah, R. *Inorg. Chem.* **1984**, *23*, 2561−2563.

Table 1. Chemical Shifts of Pyrrole and Phenyl Protons of Fe(III), Fe(IV), and Fe(III) Macrocycle Radicals Having Various Spin States and Coupling Patterns

complex	solvent	Fe spin state, S	ligand spin state, S	coupling	T (K)	δ_{pyrr}	δ_o	δ_m	δ_p	$\delta_m - \delta_p$[a]	$\delta_m - \delta_o$[a]	ref
High-Spin Fe(III) Porphyrinates												
TPPFeCl	toluene-d_8	$^5/_2$			298	+81	+7.7, +5.1	+12.7, +11.6	+6.2	+6.0	+5.8	48
TPCFeCl	$CDCl_3$	$^5/_2$			315	+82, +73, +63, (−4)[b]	+8 to +2	+11, +10, +13, +11	∼+7	∼+5	∼+6	50
$[TPPFe(DMSO)_2]ClO_4$	DMSO-d_6	$^5/_2$			295	+73	+12.9	+9.6	+9.8	−0.2	−3.3	51
Spin-Admixed Fe(III) Porphyrinates												
OETPPFeCl	CD_2Cl_2	$^5/_2$,$^3/_2$			295	—[c](36.2)[d]	+10.8, 8.2	+13.2, 13.0	+7.1	+6.0	+2.6	52
$[TPPFeO_2CCF_3]$	$CDCl_3$	$^5/_2$,$^3/_2$			302	+74.0	+8.1	+12.9, 11.9	+6.9	+5.5	+4.3	53
$[TPPFeO_3SCF_3]$	$CDCl_3$	$^5/_2$,$^3/_2$			302	+39.3	∼+7−8	+12.5	+7.5	+5.0	+5.5−4.5	53
$[TPPFeClO_4]$	$CDCl_3$	$^3/_2$,$^5/_2$			302	+13.0	+9.2	+11.9	+7.7	+4.2	+2.7	54
Intermediate Spin Fe(III) Porphyrinates												
$[(2,4,6\text{-}(OMe)_3)_4TPPFe(THF)_2]ClO_4$	$CDCl_3$	$^3/_2$			302	−28.0	—[c](+3.6)[e]	+9.2	—[c](+6.0)[e]	—[c](−sm)[f]	—[c](+sm)[f]	56
$[(2,4,6\text{-}(OMe)_3)_4TPPFeClO_4]$	CD_2Cl_2	$^3/_2$			302	−30.6	—[c](+3.5)[e]	+9.1	—[c](+4.7)[d]	—[c](−sm)[f]	—[c](+sm)[f]	56
Low-Spin Fe(III) Porphyrinates, Electron Configuration $(d_{xy})^2(d_{xz},d_{yz})^3$												
$[TPPFe(4NMe_2Py)_2]^+$	$CDCl_3$	$^1/_2$			213	−29.5	+2.4	+5.4	+5.3	+0.1	+3.0	58
$[TPCFe(4NMe_2Py)_2]^+$	CD_2Cl_2	$^1/_2$			273	0, −6.2, −32.5 (+29.6)[b]	+8 to +6	+8 to +6	+8 to+6	(−sm)[f]	(+sm)[f]	60
$[OETPPFe(4NMe_2Py)_2]^+$	CD_2Cl_2	$^1/_2$			253	—[c](+8.2)[d]	+4.0	+5.4	+6.5	−1.1	+1.4	52
$[TPPFe(ImH)_2]^+$	$CDCl_3$	$^1/_2$			298	−16.8	+5.23	+6.25	+6.32	−0.7	+1.0	51
$[TPCFe(Im\text{-}d_4)_2]^+$	CD_2Cl_2	$^1/_2$			273	−3, −7.5, −37.5 (+38)[b]	+7 to +5	+7 to +5	+7 to +5	(−sm)[f]	(+sm)[f]	60
$[OETPPFe(NMeIm)_2]^+$	CD_2Cl_2	$^1/_2$			243	—[c](+8.5)[d]	+3.8	+5.2	+6.4	−1.2	+1.4	52
$[TPPFe(p\text{-}CH_3C_6H_4)]$	toluene-d_8	$^1/_2$			213	−30	+2.3, −0.5	+3.6, +3.0	+4.8	−1.5	+2.4	61
$[TTPFe(CH_3)]$	toluene-d_8	$^1/_2$			203	−34	−1.8, +0.3	+2.2, +1.8	—[c](−1.9)[d]	—[c]	+2.8	62
$[TTPFe(CH_3)(NMeIm)]$	toluene-d_8	$^1/_2$			203	−37	−2.5, −2.9	+1.6, +1.5	—[c](−1.4)[d]	—[c]	+4.3	62
Low-Spin Fe(III) Porphyrinates, Electron Configuration $(d_{xz},d_{yz})^4(d_{xy})^1$												
$[TPPFe(4CNPy)_2]^+$	$CDCl_3$	$^1/_2$			213	−7.6	−3.5	+10.7	+5.0	+5.7	+14.2	58
$[TPPFe(t\text{-}BuNC)_2]^+$	CD_2Cl_2	$^1/_2$			298	+9.7	+1.0	+13.8	+3.2	+10.6	+12.8	38
$[p\text{-}TTPFe(2,6\text{-}XylylNC)_2]^+$	$CDCl_3$	$^1/_2$			297	+10.7	−3.4	+16.5	—[c](+12.4)[e]	—[c](+lg)[g]	+19.9	63
Fe(IV) Porphyrinates												
$[TMPFe(OCH_3)_2]$	CD_2Cl_2/5% CD_3OD	1			195	−37.5	—[c](+2.4)[e]	+7.7	—[c](+2.9)[d]	—[c](−sm)[f]	—[c](+sm)[f]	65
$[TPPFe(p\text{-}CH_3C_6H_4)Br]$	toluene-d_8	1			213	−63	+11.3, +10.9	+9.3, +9.3	+8.4	+0.9	−1.8	66
[TMPFe═O]	toluene-d_8	1			203	+8.4	—[c](+3.3,—[h])[e]	+6.4, 6.0	—[c](+2.6)[e]	—[c](−sm)[f]	—[c](+sm)[f]	60
[TMPFe═O(NMeIm)]	toluene-d_8	1			243	+4.6	—[c](+3.2,+1.6)[e]	+7.4, —[h]	—[c](2.7)[e]	—[c](−sm)[f]	—[c](+sm)[f]	69
Fe(III) Porphyrinate Radicals												
$[TPP^{\bullet}Fe(ClO_4)_2]$	CD_2Cl_2	$^5/_2$	$^1/_2$	$a_{2u}(\pi)$ uncoupled	298	+31.4	−19.3	+34.7	−12.9	+47.6	+54.0	73
$[TMP^{\bullet}Fe(ClO_4)_2]$	toluene-d_8	$^3/_2$,$^5/_2$	$^1/_2$	$a_{2u}(\pi)$ uncoupled	294	+39.6	—[c](+21.1)[d]	+58.2	—[c](+12.3)[e]	—[c](+lg)[g]	—[c](+lg)[g]	65
$[TMP^{\bullet}Fe(ClO_4)_2]$	toluene-d_8	$^3/_2$,$^5/_2$	$^1/_2$	$a_{2u}(\pi)$ uncoupled	195	+61	—[c](+39)[d]	+115	—[c](+23)[e]	—[c](+lg)[g]	—[c](+lg)[g]	65
$[TPP^{\bullet}FeCl]ClO_4$	CD_2Cl_2	$^5/_2$	$^1/_2$	$a_{2u}(\pi)$ AF coupled	299	+66.1	+34.4,37.6	−12.4	+29.5	−41.9	−48.4	74
$[TPP^{\bullet}FeCl]SbF_6$	CD_2Cl_2	$^5/_2$	$-^1/_2$	$a_{2u}(\pi)$ AF coupled	302	+66.3	+38.3	−14.7	+32.0	−46.7	−53.0	75
$[TPP^{\bullet}Fe(ImH)_2]^{2+}$	CD_2Cl_2	$^1/_2$	$^1/_2$	$a_{2u}(\pi)$ uncoupled	235	−40.1	−31.7	+30.4	−22.1	+52.5	+62.1	76
FeCl Corrolates												
[T(4-MeOP)Corr•FeCl]	CD_2Cl_2	$^3/_2$	$-^1/_2$	"$a_{2u}(\pi)$" AF coupled	303	+7.0, −3.7, −7.1, −36.4	+27.2, +26.0 +25.0, +24.8	−3.3, −3.5 −4.8, −5.2	—[c] —[c]	—[c] —[c]	−30.0 −29.9	81
[T(4-MeP)Corr•FeCl]	$CDCl_3$	$^3/_2$	$-^1/_2$	"$a_{2u}(\pi)$" AF coupled	—[i]	+5.8, −5.4, −7.3, −41.5	+26.0, +24.7 +23.9	−3.2, −3.4 −4.5, −4.7	—[c] —[c]	—[c] —[c]	−28.7 −28.5	9

[TPCorr•FeCl]	CD_2Cl_2	$^3/_2$	$-^1/_2$[i]	"$a_{2u}(\pi)$" AF coupled	303	+6.7, −4.9, −6.5, −39.1	+24.7, +23.6 +22.7	−2.3, −2.5 −3.5, −3.6	+19.4 +17.1	−21.8 −20.7	−26.6 −26.3	81
[TPCorr•FeCl]	$CDCl_3$	$^3/_2$	$-^1/_2$	"$a_{2u}(\pi)$" AF coupled	303	+6.0, −5.8, −7.0, −41.1	+25.2, +24.0 +23.1	−2.6, −2.8 −3.7, −3.8	+19.6 +17.3	−22.3 −21.1	−27.3 −26.9	9
[T(4-CF_3P)Corr•FeCl]	$CDCl_3$	$^3/_2$	$-^1/_2$	"$a_{2u}(\pi)$" AF coupled	—[i]	+5.6, −6.3, −6.8, −39.8	+24.0, +22.8 +22.0	−1.8, −2.0 −2.8, −2.9	—[e] —[e]	—[e] —[e]	−25.3 −24.9	9
[T(4-NO_2P)Corr•FeCl]	CD_2Cl_2	$^3/_2$	$-^1/_2$	"$a_{2u}(\pi)$" AF coupled	303	+6.7, −5.3, −6.5, −37.2	+22.9, +21.9 +20.8	−1.5, −1.8 −2.7, −2.8	—[e] —[e]	—[e] —[e]	−24.1 −23.6	81
[T(2,6-Cl_2P)Corr•FeCl]	$CDCl_3$	$^3/_2$	$-^1/_2$	"$a_{2u}(\pi)$" AF coupled	—[i]	+6.6, −3.8, −8.9, −37.5	—[e]	−2.9, −3.3 −4.3, −4.8	+10.0 +9.7	−13.1 −14.3	—[e] —[e]	87
[T(F_5P)Corr•FeCl]	C_6D_6	$^3/_2$	$-^1/_2$	"$a_{2u}(\pi)$" AF coupled	—[i]	−2.5, −3.1, −12.1, −33.6	—[e]	—[e]	—[e]	—[e]	—[e]	86
[T(F_5P)Corr•FeCl]	CD_2Cl_2	$^3/_2$	$-^1/_2$	"$a_{2u}(\pi)$" AF coupled	294	+3.0, −3.7, −12.6, −36.0	—[e]	—[e]	—[e]	—[e]	—[e]	81
Fe(III) Corrolates												
[T(F_5P)CorrFe(Py)$_2$]	Py-d_5	$^1/_2$			—[i]	+3.2, −61.1, −65.8, −134.6	—[e]	—[e]	—[e]	—[e]	—[e]	87
[T(F_5P)CorrFe(OEt_2)$_2$]	C_6D_6	$^3/_2$			—[i]	+19.7, +13.4, −60.0, −126.0	—[e]	—[e]	—[e]	—[e]	—[e]	87

[a] Average shift of *meta*- and/or *ortho*-H used. [b] Pyrrolene protons. [c] H not present at this position. [d] Average methylene-H shift. [e] Methyl-H shift. [f] +sm or −sm = expected to be positive or negative, respectively, but small. [g] +lg or −lg = expected to be positive or negative, respectively, and large. [h] Two resonances expected, but only one reported. [i] Temperature of the measurement not reported. [j] Shown by DFT calculations to be ClFe(III) $Corr^{-2}$•.[81]

electrons for the $S = {}^3/_2$ case but only one for the $S = {}^1/_2$ case (Table 1).

For low-spin Fe(III), there are two possible electronic ground states, as shown in Figure 1. For the more common $(d_{xy})^2(d_{xz},d_{yz})^3$ electron configuration, there is one d_π unpaired electron. In this case, as already suggested two paragraphs above, the pyrrole-H resonance has a negative chemical shift, −16.8 ppm at 25 °C for $[TPPFe(ImH)_2]^+$ (Figure 10A), and the *meso*-phenyl-H shift differences, $\delta_m - \delta_p$, and $\delta_m - \delta_o$, are small negative, and small positive, respectively.[51,57] Similar patterns are observed for TPPFe(III) complexes with other axial ligands that give rise to this electronic ground state, including high-basicity pyridine ligands,[58,59] for chlorins with the same axial ligands,[60] for porphyrinates which are highly saddled,[52] and for five-coordinate aryliron(III)[61] and alkyliron(III)[62] porphyrinates, as well as for the alkyliron-*N*-methylimidazole complexes,[62] all of which are low-spin with one d_π unpaired electron. This pattern is indicative of relatively large spin density at the pyrrole β-carbons and small (or zero) spin density at the *meso*-carbons, as expected for delocalization to the $3e(\pi)$ orbitals.

For the less common $(d_{xz},d_{yz})^4(d_{xy})^1$ electronic ground state, the d_π orbitals are filled, but the d_{xy} unpaired electron can engage in spin delocalization to the porphyrinate ring if that ring is ruffled, and such ruffling is quite extreme in many of these complexes.[8,46,63] In line with this, the pyrrole-H chemical shift is close to its diamagnetic value, or even somewhat more positive, while the *meso*-phenyl-H shift differences, $\delta_m - \delta_p$, and $\delta_m - \delta_o$, are both large and positive (+12 to +19 ppm at ambient temperatures) (Figure 11), indicating large positive spin density at the *meso*-carbons[8,38,46,59,63] (Table 1). In fact, it is interesting that the saddled complex, octaethyltetraphenylporphyrinatoiron(III) bis(t-butylisocyanide), which will be discussed in more detail elsewhere,[64] has much smaller *meso*-phenyl shifts because of the reduced possibility of ruffling of the porphyrinate ring.

For Fe(IV) porphyrinates, there have been only a few different types of complexes reported. One of these, the bis-(methoxide) complex of Fe(IV), $[TMPFe(OCH_3)_2]$,[65] has a large negative pyrrole-H chemical shift (−37.5 ppm at −78 °C, Table 1) and a *meta*-phenyl-H shift (+7.7 ppm) very close to that expected for a diamagnetic complex. Although the *ortho*- and *para*-phenyl substituents are not protons, it is clear that if they were, the shift differences, $\delta_m - \delta_p$, and $\delta_m - \delta_o$, would be quite small. The pyrrole-H and *meta*-H shifts are probably more consistent with an electron configuration $(d_{xz},d_{yz})^3(d_{xy})^1$, for at the much lower temperature of the NMR measurements than of those for the "pure" $S = {}^3/_2$ complexes discussed above, the pyrrole-H chemical shift is

(57) La Mar, G. N.; Walker, F. A. *J. Am. Chem. Soc.* **1973**, *95*, 1782−1790.
(58) La Mar, G. N.; Bold, T. J.; Satterlee, J. D. *Biochim. Biophys. Acta* **1977**, *498*, 189−207.
(59) Safo, M. K.; Gupta, G. P.; Watson, C. T.; Simonis, U.; Walker, F. A.; Scheidt, W. R. *J. Am. Chem. Soc.* **1992**, *114*, 7066−7075.
(60) Cai, S. Ph.D. Dissertation, University of Arizona, 2001.
(61) Balch, A. L.; Renner, M. W. *Inorg. Chem.* **1986**, *25*, 303−307.
(62) Arasasingham, R. D.; Balch, A. L.; Cornman, C. R.; Latos-Grazynski, L. *J. Am. Chem. Soc.* **1989**, *111*, 4357−4363.
(63) Simonneaux, G.; Schünemann, V.; Morice, C.; Carel, L.; Toupet, L.; Winkler, H.; Trautwein, A. X.; Walker, F. A. *J. Am. Chem. Soc.* **2000**, *122*, 4366−4377.
(64) Yatsunyk, L.; Walker, F. A. Manuscript in preparation.
(65) Groves, J. T.; Quinn, R.; McMurry, T. J.; Nakamura, M.; Lang, G.; Boso, B. *J. Am. Chem. Soc.* **1985**, *107*, 354−360.

fairly consistent with only one d_π unpaired electron (see also next paragraph).

Another group of well-characterized compounds consists of the phenyl complexes of Fe(IV), such as $[TPPFe(p\text{-}CH_3C_6H_4)]^+$, which has a pyrrole-H chemical shift of −63 ppm at −60 °C and *meso*-phenyl-H shift differences, $\delta_m - \delta_p$, and $\delta_m - \delta_o$, that are small positive for $\delta_m - \delta_p$ and small negative for $\delta_m - \delta_o$[66] (Table 1), indicating a mainly pseudocontact contribution to the phenyl-H, of opposite sign than that for the corresponding phenyl−Fe(III) complex. It should be noted that the pyrrole-H chemical shift (−63 ppm at −60 °C, Table 1)[66] of this complex is much more negative than that for the bis(methoxide) complex discussed in the previous paragraph, suggesting a different electron configuration for the phenyl complex, i.e., $(d_{xy})^2(d_{xz},d_{yz})^2$, with two unpaired d_π electrons.

The other Fe(IV) complexes, which contain the ferryl, $(Fe{=}O)^{2+}$, center, TMPFe(O),[67−70] have a very different pattern of proton chemical shifts: +8.4 ppm for the pyrrole-H and +6.4, +6.0 ppm for the two inequivalent types of *meta*-H at −70 °C.[69] A similar pattern is observed for the *N*-methylimidazole adduct of this species (Table 1).[69] This pattern of small upfield shifts for both types of protons is unlike that predicted for any distribution of metal d electrons, and it likely results from most of the spin density being delocalized to the oxo group, rather than the porphyrin ring. In fact, theoretical calculations of some 20 years ago indicated that the small upfield nature of both pyrrole-H and *meso*-H isotropic shifts is consistent with most of the spin density being on the oxo group.[71,72] Hence, in terms of observed chemical shifts, the ^{1}H NMR spectra of oxoiron(IV) porphyrinates behave more like diamagnetic d^6 Fe(II) bound to a six-electron (two unpaired) oxygen atom, rather than paramagnetic d^4 Fe(IV) centers.[67−72]

The Interesting Cases of Macrocycle Radicals

Instead of creation of Fe(IV) porphyrinates upon one-electron oxidation of Fe(III) porphyrinates, it is possible that the electron may be removed from the macrocycle rather than the metal. Hence, there have been a number of reports of the ^{1}H NMR spectra of Fe(III) porphyrinate radicals having various spin states and coupling schemes. For simplicity, we will concentrate on the TPPFe(III) π cation radicals, although the TMP analogues are more stable; the chemical shifts of several of these are also listed in Table 1.

For six-coordinate complexes with two weak-field perchlorate ligands, in which the metal is in the plane of the porphyrinate ring and the metal is believed to have spin state $S = {}^5/_2, {}^3/_2$, the pyrrole-H chemical shift at 25 °C is +31.4 ppm, and the *meso*-phenyl-H shift differences, $\delta_m - \delta_p$, and $\delta_m - \delta_o$, are both quite large and *positive*[73] (Table 1), indicating *positive* spin density on the porphyrinate ring. Consistent with this, the magnetic moment of this complex, $\mu_{eff} = 6.5 \pm 0.2\ \mu_B$,[73] indicates six unpaired electrons, with the metal and macrocycle unpaired electrons either uncoupled or weakly ferromagnetically coupled. The structure of the complex shows that its porphyrinate ring is planar.[73]

In contrast, for five-coordinate chloroiron(III) porphyrinate radical complexes such as $[TPPFeCl]^+ClO_4^-$, the pyrrole-H chemical shift is +66 ppm, and the *meso*-phenyl-H shift differences, $\delta_m - \delta_p$, and $\delta_m - \delta_o$, are both quite large and *negative*[74,75] (Table 1), indicating *negative* spin density on the porphyrinate ring. Consistent with this, the magnetic moment of the $SbCl_6^-$ counterion complex, $\mu_{eff} = 4.9\ \mu_B$,[73,75] indicates four unpaired electrons, i.e., *antiferromagnetic* coupling between the $S = {}^5/_2$ Fe(III) and the $S = {}^1/_2$ porphyrinate radical. It is also found to have a strongly saddled porphyrinate ring.[73]

Yet another Fe(III) porphyrinate cation radical complex is that of the low-spin Fe(III) complex $[TPPFe(ImH)_2]^{2+}$, which has a pyrrole-H shift of −40.1 ppm at −38 °C, and the *meso*-phenyl-H shift differences, $\delta_m - \delta_p$, and $\delta_m - \delta_o$, are both quite large and *positive*[76] (Table 1), indicating *positive* spin density on the porphyrinate ring. Consistent with this, the magnetic moment of the complex ($\mu_{eff} = 2.8 \pm 0.2\ \mu_B$)[76] indicates two unpaired electrons (one on the metal and one on the ring).

To understand the coupling schemes that give rise to the above shifts, we begin by noting that an unpaired electron on the macrocycle will certainly be in a π symmetry orbital, most likely the HOMO of the macrocycle, due to loss of one electron from that orbital; hence, metalloporphyrinate radicals are often called "π cation radicals" because one electron has been removed from the π system of the macrocycle, and it thus has a charge that is one oxidation state higher than its normal charge (−2 for a porphyrinate), hence a −1 charge for a porphyrinate. For tetraphenylporphyrinates, the HOMO is the $3a_{2u}(\pi)$ orbital, shown in Figure 2. Thus, it is the $3a_{2u}(\pi)$ orbital from which a porphyrinate electron will be removed. This orbital is not of the proper symmetry to interact with any of the d orbitals if the porphyrinate ring is planar, as is the case for the six-coordinate complexes, both the $S = {}^5/_2, {}^3/_2$ Fe(III) cation radical bis(perchlorate) and the $S = {}^1/_2$ Fe(III) bis(imidazole) complexes. Hence, in these cases the metal and macrocycle unpaired electrons are either not coupled at all, or else are weakly ferromagnetically coupled; it is difficult to tell the difference between these possibilities if one has available only magnetic moments measured in solution by the Evans method.[77] The spin density distribution in the porphyrinate ring of these radicals is shown in Figure 9e. In contrast, in the five-coordinate complex having a very saddled porphyrinate core, it would be symmetry-allowed, as pointed out by the authors,[73] for this porphyrinate ring conformation to

(66) Balch, A. L.; Renner, M. W. *J. Am. Chem. Soc.* **1986**, *108*, 2603−2608.
(67) Chin, D. H.; Balch, A. L.; La Mar, G. N. *J. Am. Chem. Soc.* **1980**, *102*, 1446−1448.
(68) La Mar, G. N.; de Ropp, J. S.; Latos-Grazynski, L.; Balch, A. L.; Johnson, R. B.; Smith, K. M.; Parish, D. W.; Cheng, R. J. *J. Am. Chem. Soc.* **1983**, *105*, 782−787.
(69) Balch, A. L.; Chan, Y.-W.; Cheng, R.-J.; La Mar, G. N.; Latos-Grazynski, L.; Renner, M. W. *J. Am. Chem. Soc.* **1984**, *106*, 7779−7785.
(70) Balch, A. L.; La Mar, G. N.; Latos-Grazynski, L.; Renner, M. W.; Thanabal, V. *J. Am. Chem. Soc.* **1985**, *107*, 3003−3007.
(71) Loew, G. H.; Herman, Z. S. *J. Am. Chem. Soc.* **1980**, *102*, 6114−6115.
(72) Hanson, L. K.; Chang, C. K.; Davis, M. S.; Fajer, J. *J. Am. Chem. Soc.* **1981**, *103*, 663−670.
(73) Buisson, G.; Deronzier, A.; Duée, E.; Gans, P.; Marchon, J.-C.; Regnard, J.-R. *J. Am. Chem. Soc.* **1982**, *104*, 6793−6795.
(74) Phillippi, M. A.; Goff, H. M. *J. Am. Chem. Soc.* **1982**, *104*, 6026−6034.
(75) Gans, P.; Marchon, J.-C.; Reed, C. A.; Regnard, J.-R. *Nouv. J. Chim.* **1981**, 203−204.
(76) Goff, H. M.; Phillippi, M. A. *J. Am. Chem. Soc.* **1983**, *105*, 7567−7571.
(77) Evans, D. F. *J. Chem. Soc.* **1959**, 2003−2005.

make possible antiferromagnetic coupling of the $d_{x^2-y^2}$ unpaired electron of the high-spin Fe(III) center with the $3a_{2u}(\pi)$ unpaired electron to yield negative spin density on the porphyrinate ring. The spin density distribution in the porphyrinate ring of these radicals is shown in Figure 9f.

The Special Case of Iron Corrolates

Corroles are tetrapyrrole macrocycles that are related to porphyrins, except that they lack one *meso*-carbon, and, in order to retain the same number of π electrons, are thus, when fully deprotonated, trianionic ligands for transition metal ions. They have unique properties, including the capability of maintaining a planar conformation, the possibility of stabilizing high oxidation states for coordinated metal ions,[78] and/or the possibility of stabilizing a one-electron oxidized macrocycle.[79] We have reported NMR and EPR spectroscopic studies of two chloroiron octaalkylcorrolates ([(Me_8Corr)FeCl] and [(7,13-Me_2Et_6Corr)FeCl]) and their bis(imidazole) complexes,[79] as well as their complex formation with, and autoreduction by, cyanide ion.[80] We have also recently reported the investigation of a series of chloroiron triphenylcorrolates by ^{1}H and ^{19}F NMR spectroscopy;[81] the ^{1}H NMR spectra of several chloroiron triphenylcorrolates have also been reported by Ghosh and coworkers.[9] The results of all of these studies have shown unambiguously that these five- and six-coordinate iron corrolates are actually iron(III) corrolate(2−•) π cation radicals,[79,80] and that axial ligands such as cyanide can readily autoreduce the corrolate radical, leaving a low-spin Fe(III) mono(cyanide) complex.[80] The nature of the magnetic coupling between the unpaired electrons on the metal and the corrolate(2−•) π cation radical differs, depending on the axial ligand(s) present: Very strong antiferromagnetic coupling is observed in the case of the chloride complexes (as evidenced by the fact that the *meso*-H resonances are found at +187(1) and +174(2) ppm at 300 K, which can only occur when there is *large negative* spin density at the *meso*-carbons, as shown in Figure 9f, to the point of the C_m position).[79] In contrast, uncoupled or weak ferromagnetic coupling is observed in the case of the imidazole complexes,[79] and stronger ferromagnetic coupling in the case of the bis(cyanide) complex, [(7,13-Me_2Et_6Corr)Fe$(CN)_2]^-$.[80] However, in all cases, the corrole π orbital used for the macrocycle unpaired electron is the $7b_1$ orbital,[4,82] which is analogous to the $3a_{2u}(\pi)$ orbital of the porphyrin ring.[4] This orbital has large π spin density at the *meso*-carbon positions and negligible spin density at the pyrrole β-carbons.[4,79,82]

We have recently published a detailed study[10] that fully corroborates the earlier interpretations of the NMR data for the chloroiron octaalkylcorrolates,[79] in which several experimental techniques (magnetic susceptibility measurements, Mössbauer, and NMR spectroscopy), as well as DFT calculations, were used to establish unambiguously the electron configuration and spin density distributions of the

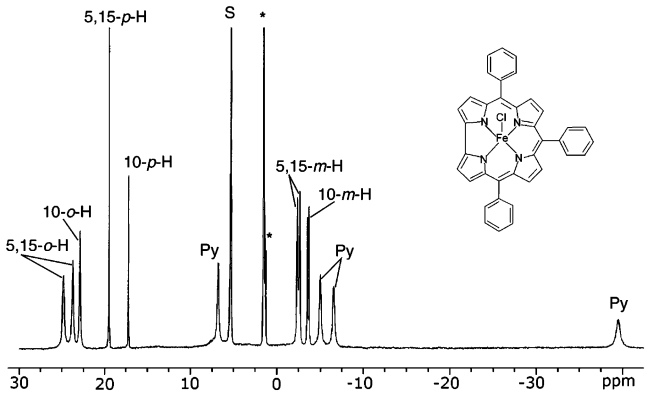

Figure 12. 1D ^{1}H NMR spectrum of [TPCorrFeCl] in CD_2Cl_2 at 298 K.[81] The solvent resonance is marked with S, and those peaks marked with asterisks are due to impurities; pyrrole-H resonances are marked with Py. The chemical shifts (and their range) should be compared and contrasted with those of Figure 9. Reprinted from ref 81, copyright 2002, with permission of Elsevier.

chloroiron octaalkyl- and triphenylcorrolates, as well as the phenyliron octaalkylcorrolate.[10] In all of the chloroiron complexes, the NMR spectra were strongly indicative of an electron configuration in which the metal is $S = {}^3/_2$ Fe(III) and the corrolate macrocycle is a cation radical, $Corr^{2-\bullet}$.[10,79,81] This conclusion was reached by analysis of the *meso*-H chemical shifts of the octaalkylcorrolates (large, positive shifts, indicating negative spin density at the *meso*-carbons, Figure 9f)[79,10] and the *meso*-phenyl-H chemical shifts of the triphenylcorrolates, as shown in Figure 12 (large negative shifts of the *meso-meta*-H, large positive shifts of the *meso-ortho*- and *para*-H, yielding $\delta_m - \delta_p$ and $\delta_m - \delta_o$ both large and negative, Figure 9f),[81] as summarized in Table 1. (It is interesting to note that there are fairly large solvent effects on the chemical shifts of these complexes, as evidenced by the entries for [TPCorrFeCl][9,81] in CD_2Cl_2 and $CDCl_3$ and those for [T(F_5P)CorrFeCl][81,86] in C_6D_6 and CD_2Cl_2. At the present time, these solvent effects have not been explained.) It is instructive to compare the spectra shown in Figures 11 ($[TPPFe(t\text{-}BuNC)_2]^+$, with *positive* spin density at the *meso*-carbons[38]) and 12 ([TPCorrFeCl], with *negative* spin density at the *meso*-carbons[81]), to see the difference in sign and magnitude of the phenyl-H shifts and the chemical shift(s) of the pyrrole-H (marked Py in Figure 12). The spin density diagrams of Figure 9c,f should also be compared.

In contrast to all of the chloroiron complexes, for the phenyliron complex of the octaalkylcorrolate, the *meso*-H shifts are still large and positive (+ 53.4 and +49.4 ppm at 303 K), although only about 25% as large as those of the chloroiron complexes.[10] DFT calculations for the chloroiron and phenyliron corrolates showed that the chloroiron corrolates have negative spin density at each *meso*-carbon of approximately −0.25, and alternating sign spin density at the other aromatic carbons of the corrolate ring, the sum of which is approximately −0.7 to −0.8, Figure 13A,B, indicating an approximate Fe(III) corrolate(2−•) π cation radical electron configuration. In comparison, the phenyliron corrolate has negative spin density at each *meso*-carbon of

(78) Licoccia, S.; Paolesse, R. *Struct. Bonding* **1995**, *84*, 71−133.
(79) Cai, S.; Walker, F. A.; Licoccia, S. *Inorg. Chem.* **2000**, *39*, 3466−3478.
(80) Cai, S.; Licoccia, S.; Walker, F. A. *Inorg. Chem.* **2001**, *40*, 5795−5798.
(81) Cai, S.; Licoccia, S.; D'Ottavi, C.; Paolesse, R.; Nardis, S.; Bulach, V.; Zimmer, B.; Shokhireva, T. Kh.; Walker, F. A. *Inorg. Chim. Acta* **2002**, *339C*, 171−178.
(82) Hush, N. S.; Dyke, J. M.; Williams, M. L.; Woolsey, I. S. *J. Chem. Soc., Dalton Trans.* **1974**, 395−399.
(83) Ghosh, A.; Steene, E. *JBIC, J. Biol. Inorg. Chem.* **2001**, *6*, 739−752.
(84) Ghosh, A.; Steene, E. *J. Inorg. Biochem.* **2002**, *91*, 423−436.
(85) Johansson, M. P.; Sundholm, D.; Gerfen, G.; Wikström, M. *J. Am. Chem. Soc.* **2002**, *124*, 11771−11780.
(86) Simkhovich, L.; Goldberg, I.; Gross, Z. *Inorg. Chem.* **2002**, *41*, 5433−5439.

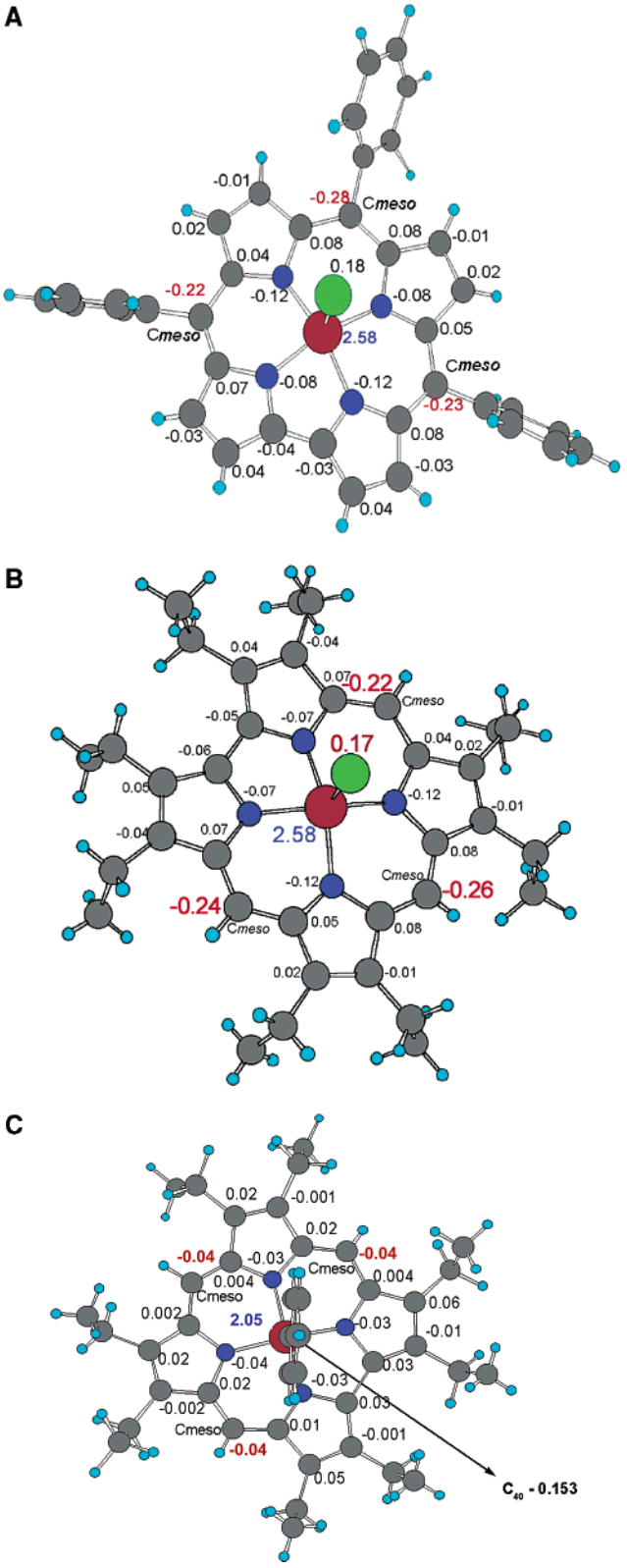

Figure 13. Calculated spin densities for [TPCorrFeCl] (a), [OECorrFeCl] (b), and [OECorrFePh] (c), showing the patterns of negative and positive spin density on the corrolate macrocycle in each case.[10] Reprinted with permission from ref 10. Copyright 2002 American Chemical Society.

approximately −0.04, and alternating sign spin density at the other aromatic carbons of the corrolate ring, the sum of which is zero, within experimental error, Figure 13C, indicating an approximate Fe(IV) corrolate(3−).[10] However, *even in this case, the corrolate ring certainly is not "innocent", in that there is significant positive and negative spin density distributed around the ring*, in an alternating manner.[10] It thus appears that the odd number of atoms in this macrocycle ring causes a very nontraditional distribution of spin density for both chloroiron and phenyliron corrolates. Similar patterns of alternating positive and negative spin densities, although smaller in magnitude in each case, have been obtained from DFT calculations on the chloroiron corrolates by Ghosh and co-workers.[9,83,84] Such alternating signs of spin densities have not been observed in iron porphyrinates, although recent DFT calculations by Johansson and co-workers suggest that in low-spin Fe(III) porphyrinates the sign of the spin density on the nitrogens is negative.[85] It may be that a simple way of viewing the very noninnocent corrolate macrocycle is that since there is an odd number of atoms in the corrolate ring, it behaves as an odd-alternant hydrocarbon in many, if not all, of its complexes.

It has been stated that the electron configuration of all (anion) iron corrolates is Fe(IV) corrolate(3−), and a recent paper, entitled in part, "...and no indications for corrole radicals",[86] claims to provide proof that the electron configuration of chloroiron(tripentafluorophenyl)corrolate and -(tri(2,6-dichlorophenyl))corrolate are unambiguously Fe(IV) corrolate(3−) electron configurations. However, the presentation involves a misinterpretation of the NMR data provided in Table 3 of that paper, which should have been caught by the reviewers: (1) Only the absolute value of the difference in chemical shift between *meso*-*meta*-phenyl-H and -*para*-phenyl-H was considered, rather than both the magnitude *and sign*, as presented in Table 1 and Figure 9c,e,f herein; (2) the decision as to electron configuration was based totally upon the chemical shift pattern of the oxoiron(IV) (ferryl) complex of tetramesitylporphyrin, which has been shown not to be a "typical" metal-based unpaired electron system;[71,72] and (3) it is claimed that the pyrrole-H shifts are most diagnostic of the spin state. With regard to the latter statement, *both* $S = 1$ Fe(IV) and $S = {}^3/_2$ Fe(III) are likely to have *two* d_π unpaired electrons, and hence, the chemical shifts of the pyrrole-H of both of these spin states should be similar (the alternative being that one or the other has only one d_π unpaired electron and hence half the hyperfine shift of the other, or that both have only one d_π unpaired electron and are hence very similar to low-spin Fe(III) with the $(d_{xy})^2(d_{xz},d_{yz})^3$ ground state discussed above). And as we have seen above, Fe(IV) porphyrinates having two d_π unpaired electrons have pyrrole-H chemical shifts of about −63 ppm at −60 °C,[66] or roughly −30 to −35 ppm at room temperature (hyperfine shifts of −39 to −44 ppm). This value matches well the pyrrole-H chemical shift of $(2,4,6\text{-}(OCH_3)_3)_4$-TPPFeOClO$_3$ at 25 °C (−30 ppm; hyperfine shift of −39 ppm)[56] and is approximately double the hyperfine shift observed for low-spin Fe(III) porphyrinates having a $(d_{xy})^2(d_{xz},d_{yz})^3$ electron configuration, which have only one d_π unpaired electron (chemical shift ∼ −16 ppm, hyperfine shift ∼ −25 ppm)[51,57] (the chemical shifts of all of these species are summarized in Table 1). Hence, as pointed out previously,[81] pyrrole-H shifts are *not* diagnostic of the spin state of these chloroiron corrolates. Rather, the *meso*-H or *meso*-phenyl-H shifts are by far the most diagnostic, because they provide evidence for the presence or absence of negative spin density at the *meso*-carbons. Similarly, for the antiferromagnetically coupled chloroiron porphyrinate radicals

discussed in the previous section, the pyrrole-H shifts are not all that much different from those of other high-spin Fe(III)-containing porphyrinate systems, whereas the *meso*-phenyl shift differences are much larger and negative (+5 to +6 ppm for chloroiron porphyrinates[48,50,52,53] as compared to −42 to −53 ppm for antiferromagnetically coupled chloroiron porphyrinate radicals[74,75]).

The chemical shifts of all of the chloroiron triphenylcorrolates that have been reported thus far,[9,81,86,87] included in Table 1, all have extremely similar pyrrole-H chemical shifts, with widely spaced resonances ranging from +6/+3 to −33/−39 ppm. Although some of the shifts are reported at unspecified temperatures close to ambient, their wide range of chemical shifts for the pyrrole-H of a given complex indicates widely varying spin density at the pyrrole carbons within a given compound, yet a very similar range of shifts from one compound to another. More to the point, the *meso*-phenyl-H shift differences of the 2,6-dichlorophenyl complex, $\delta_m - \delta_p$ and $\delta_m - \delta_o$, are large and *negative*,[87] as is the case for all other substituted phenyl chloroiron triphenylcorrolates,[9,81] indicating large negative spin density at the *meso*-carbons of all of these chloroiron corrolates. Hence, there is no basis for claims that the electron configuration of the two chloroiron triphenylcorrolates reported by one laboratory[86,87] is different from those reported by all other laboratories, and thus no basis for claims of an electron configuration of any chloroiron corrolate that is different from $S = {}^3/_2$ Fe(III) coupled antiferromagnetically to a corrolate π cation radical, as originally concluded and stated on the basis of the ^{1}H NMR spectroscopic data.[79]

The ^{19}F NMR data for the chloroiron tri(pentafluorophenyl)corrolate are not as helpful as we had hoped they would be, for the phenyl-F values do not show the alternating signs shown by phenyl-H, discussed above. For this complex, all ^{19}F isotropic shifts are negative,[81] while the isotropic shifts of all *meso*-phenyl-F bound to iron porphyrinates having positive spin density at the *meso*-carbons are positive.[88−90] However, in both cases the shifts are smaller than might have been expected, and they do not show alternating signs for *ortho*- and *para*-F as compared to *meta*-F. Nevertheless, the sign difference between the chloroiron tri(pentafluorophenyl)-corrolate[81] and chloroiron tetra(pentafluorophenyl)porphyrinate[88] is consistent with negative spin density at the *meso*-carbons of the corrolate.[88] However, it is at this time not possible to use ^{19}F shifts to determine the *amount* of spin density present at the *meso*-carbons; significantly more ^{19}F shifts of paramagnetic metal complexes must be reported and carefully analyzed before this will be possible.

The ^{1}H chemical shifts of two complexes of the one-electron reduced state of the chloroiron tri(pentafluorophenyl)corrolate, [T(F$_5$P)CorrFeL$_2$], where L = pyridine or diethyl ether, have also been reported.[86] The ^{1}H chemical shifts of each of these are included at the end of Table 1. In both cases, the pyrrole-H chemical shifts are highly anomalous, on the basis of our expectations from the data for iron(III) porphyrinates. This can clearly be seen by comparing the spread and average pyrrole-H shifts of the pyridine complex of the supposed iron(III) tri(pentafluorophenyl)-corrolate (137.8, −64.6 ppm, respectively) to that of the bis(4-(dimethylamino)pyridine) and -(imidazole) complexes of another similarly lower-symmetry macrocycle, tetraphenylchloriniron(III) (32.5, −12.9 and 34.5, −16.0 ppm, respectively.)[60] For the bis(diethyl ether) complex of the same Fe(III) corrolate, the pyrrole-H chemical shifts are even more anomalous, with two resonances having large positive chemical shifts (+19.7, +13.4 ppm) and two having large negative chemical shifts (−60.0 and −126.0 ppm), yielding a spread of 145.7 ppm and an average pyrrole-H shift of −38.2 ppm. While it has been claimed that this pattern is indicative of an $S = {}^3/_2$ intermediate spin state Fe(III) center,[86] *there is no precedent in the literature for having both large positive and large negative chemical shifts of protons directly attached to the π system of any "innocent" macrocycle*. It is not possible for any spin state of either an Fe(III) or Fe(IV) *porphyrinate* complex to have large positive spin density at two, and large negative spin density at the other two, pyrrole-H positions. Hence, the large positive and large negative chemical shifts of the pyrrole-H of this Fe(III) corrolate bis(diethyl ether) complex, if they all arise from the same species, are indicative of a *highly* noninnocent macrocycle complex. DFT calculations should be carried out on this complex to determine the spin density distribution for comparison with the ^{1}H chemical shifts.

Summary

In this Viewpoint, it is hoped that several things have been accomplished, including (1) showing that pulsed EPR spectroscopy is extremely useful both in determining the orientation of the **g**-tensor and in determining the pattern of spin delocalization (large/small) on the macrocycle ring; (2) showing that ^{1}H NMR spectroscopy is extremely useful in determining not only the pattern (large/small) of spin delocalization, but also the sign of the spin density at those positions at which protons are bound, and that these concepts can be easily grasped by students; and (3) showing that for iron corrolates the ^{1}H NMR chemical shifts are explained, both in terms of magnitude and of sign, by DFT calculations, leading to the undeniable conclusion that these macrocyclic complexes are highly noninnocent, with alternating positive and negative spin density around the corrolate ring. A more complete mapping of spin density may be obtained from ^{13}C NMR investigations, which we intend to carry out on some of the most soluble complexes soon.

Abbreviations: TPP, tetraphenylporphyrin; TPC, tetraphenylchlorin; TTP, tetratolylporphyrin; TMP, tetramesitylporphyrin; X$_4$TPP, X-substituted TPP, where X is a substituent on each of the phenyl rings; OEP, octaethylporphyrin; OETPP, octaethyltetraphenylporphyrin; Corr, corrole; TPCorr, triphenylcorrole; T(X$_n$P)Corr, tri(X-substituted phenyl) corrole; PzH, pyrazole, ImH, imidazole; Im-d_4, deuterium-substituted imidazole; NMeIm, *N*-methylimidazole; 4NMe$_2$-Py, 4-(dimethylamino)pyridine; 4CNPy, 4-cyanopyridine; t-BuNC, t-butylisocyanide; PhNC, phenylisocyanide; 2,6-XylylNC, 2,6-dimethylphenylisocyanide; DMSO, dimethyl sulfoxide; Ph, phenyl; HOMO, highest occupied molecular orbital; LUMO, lowest unoccupied molecular orbital; DFT, density functional theory.

(87) Simkhovich, L.; Galili, N.; Saltsman, I.; Goldberg, I.; Gross, Z. *Inorg. Chem.* **2000**, *39*, 2704−2705.
(88) Yatsunyk, L.; Walker, F. A. *Inorg. Chim. Acta* **2002**, *337*, 266−274.
(89) Birnbaum, E. R.; Hodge, J. A.; Grinstaff, M. W.; Schaefer, W. P.; Henling, L.; Labinger, J. A.; Bercaw, J. E.; Gray, H. B. *Inorg. Chem.* **1995**, *34*, 3625−3632.
(90) Grinstaff, M. W.; Hill, M. G.; Birnbaum, E. R.; Schaefer, W. P. Labinger, J. A.; Gray, H. B. *Inorg. Chem.* **1995**, *34*, 4896−4902.

Acknowledgment. This work has been supported by the National Institutes of Health, Grant DK31038. The author would like to thank her current and former co-workers who have carried out the pulsed EPR and ^{1}H NMR spectroscopic investigations of iron porphyrinates, chlorinates, and corrolates, most especially Liliya Yatsunyk, who recorded several spectra to provide data for Table 1, and Dr. Andrei Astashkin for helpful comments. She also wishes to thank her collaborators, Professor Alfred X. Trautwein and co-workers at the University of Lübeck, who carried out the magnetic susceptibility and Mössbauer spectroscopic measurements and DFT calculations on the iron corrolates, and Professor Silvia Licoccia and co-workers at the University of Rome Tor Vergata, who synthesized numerous samples of the iron corrolates. Helpful conversations with Professor Abhik Ghosh are also acknowledged.

IC026245P